SOCIETY OF NUCLEAR MEDICINE
AND MOLECULAR IMAGING
MIRD COMMITTEE

MIRD soft

MIRD calc

Organ-Level Dosimetry Software

User Manual

Version 1.1-Genesis

Memorial Sloan Kettering Cancer Center

UF UNIVERSITY of FLORIDA

Legal Notice

1 TABLE OF CONTENTS

2 SOFTWARE OVERVIEW

2.1 MIRDCALC

MIRDcalc is an organ level dosimetry software tool for estimating radiation dosimetry from internally distributed isotopes.

Users are encouraged to read manual thoroughly. All input parameters can/will affect output dosimetry estimates; therefore, a full understanding of input design is required by the user.

2.2 ACKNOWLEDGEMENTS

MIRDcalc version 1.0 is part of a grant supported project from the United States National Institute of Biomedical Imaging and Bioengineering, grant 5-U01-EB028234: "MIRDCalc – A Community Tool for Deriving and Reporting Patient Organ Doses in Nuclear Medicine, Computed Tomography, and Hybrid Imaging". Principle Investigators: Wes Bolch (University of Florida) and Adam Kesner (Memorial Sloan Cancer Center).

Major project contributors include: Justin Brown (UF), Lukas Carter (MSKCC), Sean J. Domal (UF), John L. Humm (MSKCC), Derek Jokisch (FMU), Ryan Kerslake (MSKCC), Cameron B. Kofler (UF), Daniel Lafontaine (MSKCC), Juan C. Ocampo Ramos (MSKCC), Edmond Olguin (UF), Bonnie N. President (UF), Trung Tran (UF) and Pat Zanzonico (MSKCC).

We acknowledge guidance and support from the Society of Nuclear Medicine and Molecular Imaging Committee on Medical Internal Radiation Dose, and the SNMMI organization.

We acknowledge author Cecilia Hindorf and the International Atomic Energy Agency for authorizing the reproduction of their nuclear medicine dosimetry educational material in the MIRDcalc User Manual (Appendix A).

3 INSTALLATION

3.1 DOWNLOADING

MIRDcalc is freely available on the MIRDsoft.org website: www.mirdsoft.org

3.2 REQUIREMENTS

The MIRDcalc software is built within the Microsoft Excel environment and compiled using XLS padlock. MIRDcalc software requires a windows PC with Microsoft Windows 7 (32- or 64-bit) or later, and Microsoft Office 2013 or later installed.

3.3 INSTALLING

The MIRDcalc installation file can be downloaded from www.MIRDsoft.org.

To install the software, launch installation file and follow instructions. Software will automatically install to the location "C:\MIRDsoft\MIRDcalc\MIRDcalc_v1.0\".

User's may need permissions and firewall exceptions from their site administrators to complete installation.

3.4 UNINSTALLING

To uninstall MIRDcalc, use the MIRDcalc uninstaller "C:\MIRDsoft\MIRDcalc\MIRDcalc_v1.0\uninsooo.exe"

3.5 TROUBLESHOOTING

We are collecting feedback from users, and will post troubleshooting advice as it is collected. These items will be posted on our website:

https://mirdsoft.org/mirdcalc-software-use-notes

4 MIRDCALC SOFTWARE

4.1 GENERAL OVERVIEW OF SOFTWARE USE

MIRDcalc is built very similarly to other available organ-level dosimetry programs – the general workflow consists of a few basic steps:

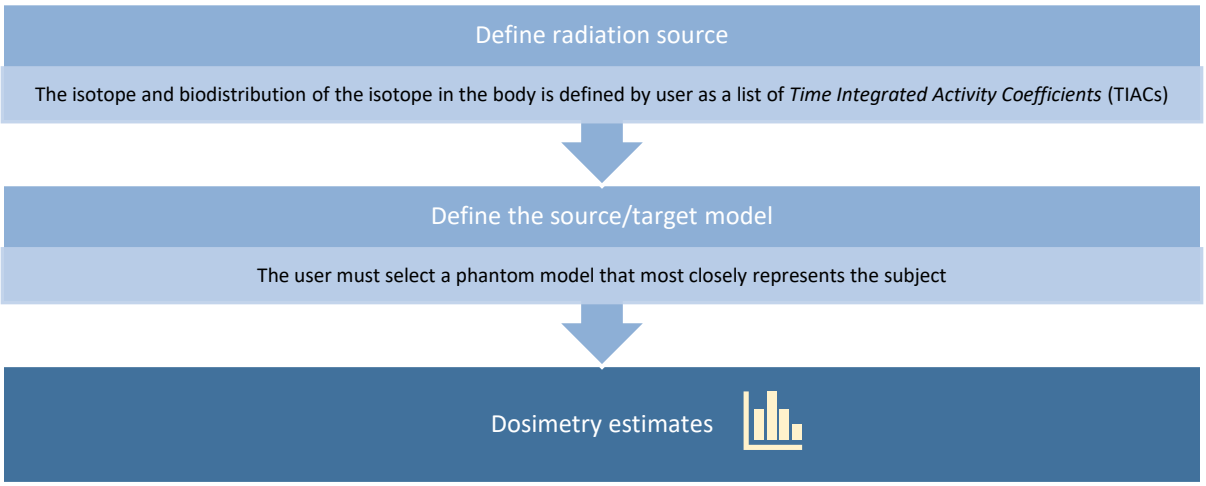

4.2 MIRDCALC INNOVATIONS

MIRDcalc was built with an aim of pushing forward dosimetry calculation capacities in the field. To this end MIRDcalc provides some innovations which include:

- Error propagation
- Phantom interpolation of S-values
- *Effective dose*, *Detriment weighed dose*, and *Risk index* calculation
- Dynamic *Rest of body* term
- Dynamic *Rest of blood* and *Rest of parenchyma* to support full accounting of blood source (New source regions to complete accounting for total blood: *Heart blood pool* and *Major blood vessels)*
- Easy to use single-screen interface
- Quality control graphics – instant dose calculations
- Fully accessible calculations (open source)
- Command line and batch processing capacity
- Thorough case documentation
- Thorough (ICRP) phantom documentation
- Free distribution
- Platform for collaborative software evolution

4.3 MIRDCALC QUICK-STEP INSTRUCTIONS FOR USE

In this handbook, instructions for performing dosimetry calculations are provided. A quick overview of steps required for internally distributed isotope dose estimation is provided below:

MIRDcalc Quick-Step Usage Summary

1. Select ***Element/Isotope***
2. Select ***Sex/Phantom***
3. Enter biodistribution TIACs
    - (optional) Enter ***Subject ID***
    - (optional) Enter estimated TIAC uncertainty
    - (optional) Modify mass of target organs, enter estimated organ mass uncertainty
    - (optional) Modify estimated global uncertainty – to account for the assumptions inherent in phantom-modelled *Organ Level Dosimetry*
    - (optional) Enter ***Waste*** TIAC
    - Review input parameters for accuracy
4. Dosimetry automatically generated on interface [units mGy/MBq]
    - (optional) Enter ***Injected activity*** – to display projected dose per injection calculation
5. Select ***Save*** to export case; *.csv (tab-delimited) format & *.pdf (pdf snapshot)

Note - An elemental understanding of the fundamentals of dosimetry is strongly encouraged for proper use of this software. Many of these concepts are presented in Appendix A.

5 DETAILED INSTRUCTIONS FOR DOSIMETRY CALCULATIONS

In MIRDcalc, dosimetry estimates are calculated based on user biodistribution input.

5.1 GENERAL INPUT INSTRUCTIONS

MIRDcalc has two types of input fields: multiple choice slicers and text fields.

Slicers – the MS Excel platform supports multiple choice selections via slicers. The user may select fields from the presented slicers.

Text fields – all yellow fields on the interface are editable. All non-yellow fields are not.

5.2 INPUTS FOR DOSE CALCULATION

MIRDcalc dose estimation works by loading a phantom-specific biodistribution-to-dose model that has been previously generated. The user supplies the patient specific biodistribution (as TIACs), ultimately generating a set of organ level dosimetry estimates for the given phantom model and patient specific biodistribution.

The process for generating estimates are as follows:

5.2.1 Element, isotope, sex, and phantom

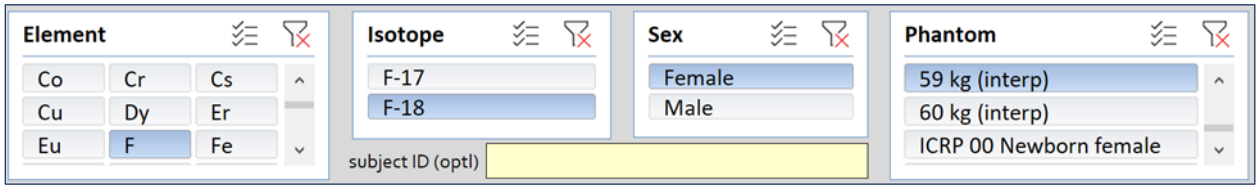

The selection of isotope, sex, and phantom loads the database information necessary to estimate dosimetry for a particular model/case - specifically the S-value library. The S-value libraries provide the dose-calculation framework for all organ source-target pairs per unit activity for a given isotope/phantom (see Appendix A). By selecting a combination of Element, Isotope, Sex, and Phantom parameters, a unique S value library will be loaded to MIRDcalc to enable calculation.

MIRDcalc has 333 unique isotopes, 2 Sexes, and 12 ICRP phantom models to choose from. In addition, the user may select a phantom model based on weight: the "XX kg (interp)" selection. This selection will load a phantom model that is an interpolation between the two closest ICRP phantoms; the organ masses are linearly interpolated between the associated values in the closest ICRP phantom models; the S values are interpolated along a power function via log-log curve fitting.

5.2.2 Biodistribution TIACs

MIRDcalc provides biodistribution-specific dosimetry estimates. To accomplish this, a characterization of the biodistribution of an isotope needs to be input into the software.

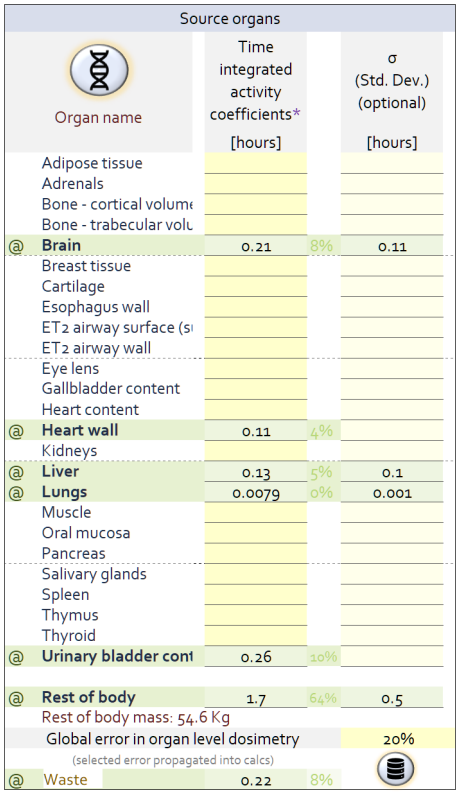

In MIRDcalc, the biodistribution (source activity) is defined by assigning *Time Integrated Activity Coefficients* (TIACs) to source organ/regions. This is accomplished by entering the TIAC values in the specified TIAC fields. Users will only enter in values for organs they can or want to define as specific sources of radioactive emissions.

The TIAC values, formerly called "residence times" in some publications, are calculated as the time-integrated activity of a source region normalized by the unit injection, and has units of time (see Appendix A). They represent the amount of isotope emissions that come from an organ – i.e. entering a TIAC value into an organ TIAC field defines a source and "strength" of radiation. In MIRDcalc, the units of TIAC should be [hours].

Deriving TIACS for dosimetry is solely up to the user. Unless specifically intended by biodistribution model, the total time of the TIACs entered into MIRDcalc should account for 100% of a unit injection, i.e. one times the integral of decay over time between zero and infinity. This is shown in equation (1)

$$TIAC_{100\%}\left\{\begin{matrix} Theoretical \\ sum\ of\ TIACs \end{matrix}\right\} = \int_{t=0}^{t=\infty} e^{\lambda t} = decay\_constant(\lambda)^{-1} = \frac{isotope\_half\_life(\tau_{1/2})}{ln\ (2)} \quad (1)$$

An example 100% TIAC calculation is presented for F-18 (1.83 hour half-life):

$TIAC_{100\%}$ (F-18) = 1.83 [hours] * 1.44 = 2.64 [hours].

TIAC data entry:

TIAC data can be entered into specific source organ source regions and MIRDcalc "*Rest of __*" source regions.

Specific organ source regions – MIRDcalc displays 25/81 source organ regions on the graphical user interface. A total of 81 possible source organ regions are available for use in MIRDcalc (see Appendix B for full list) and can be accessed using the organ selection button (see section 5.2.3).

"*Rest of* " source regions – these regions are dynamic regions used to distribute TIACs in multiple body regions and are further explained in section 6.2.

5.2.3 Organ selection

In addition to the default 25 displayed source regions on the home screen, users may access the full list of 81 possible source regions via the organ selection tab. To launch tab, click the organ selection button . User will need to confirm acceptance that the TIAC table entry data will be cleared of any entered values. At this point, the user will be shown an organ selection user interface:

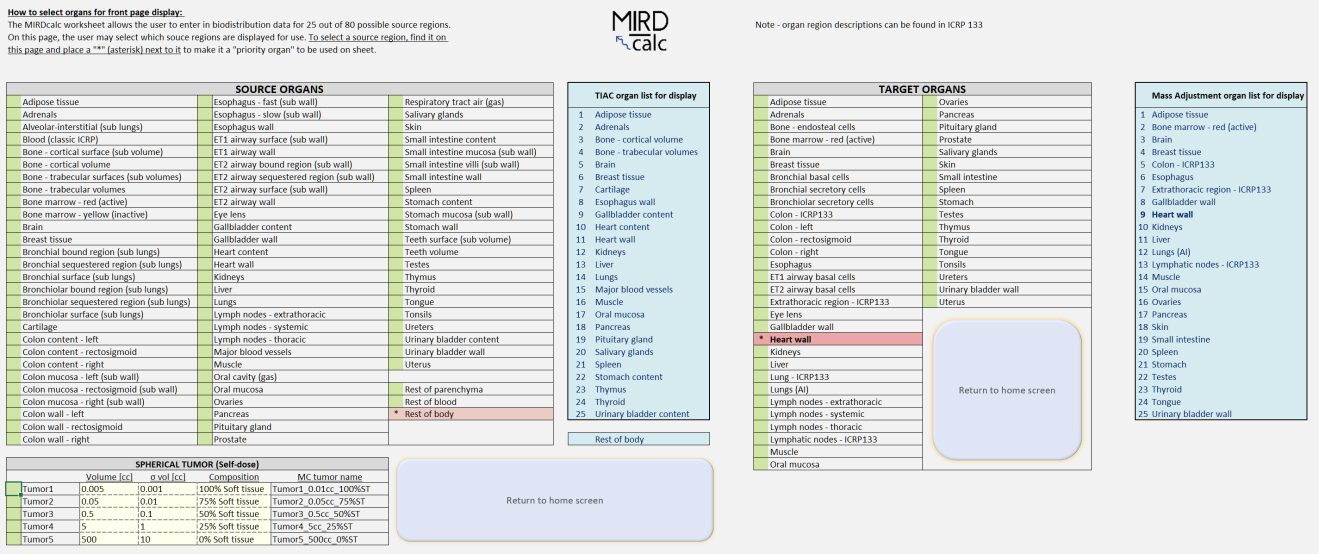

Figure 1 – screenshot of organ selection screen

To utilize any specific organ/regions on the main internal dosimetry spreadsheet for use, the user needs to place an asterisk (*) adjacent to that organ on the organ selection interface. An organ that has an asterisk (*) next to it will be given priority and added to the alphabetically organized TIAC organ list – shown in blue.

Similar organ selection is available for target regions, on the right side of the organ selection interface. Here the user may update which organs are available for mass modification on the home screen.

Once desired organs/regions are selected, the user can click "return to home screen" to return to the main internal dosimetry spreadsheet.

5.2.4 Organ selection – Tumor (sphere)

Users are able to include up to 5 spherical tumor regions in MIRDcalc source entry regions. To initiate this, the user needs to navigate to the organ selection tab (see 5.2.3), and select tumor regions for inclusion, analogous to selecting other source regions.

SPHERICAL TUMOR (Self-dose)					
		Volume [cc]	σ vol [cc]	Composition	MC tumor name
*	**Tumor1**	**0.005**	**0.001**	**100% Soft tissue**	**Tumor1_0.01cc_100%ST**
*	**Tumor2**	**0.05**	**0.01**	**75% Soft tissue**	**Tumor2_0.05cc_75%ST**
*	**Tumor3**	**0.5**	**0.1**	**50% Soft tissue**	**Tumor3_0.5cc_50%ST**
	Tumor4	5	1	25% Soft tissue	Tumor4_5cc_25%ST
	Tumor5	500	10	0% Soft tissue	Tumor5_500cc_0%ST

Figure 2 – screenshot of tumor volumes of organ selection screen

When a tumor region is selected by placing an asterix ("*") next to it, the user needs to set the tumor's **volume**, **volume uncertainty (optional)**, and **composition** (% soft tissue vs % mineral bone). The tumor regions are defined as isolated spheres, and can be used to calculate dose for a given volume, isotope, and composition.

MIRDcalc supports calculations for tumor volumes between 0.004 cc – 3000 cc.

The methodology for tumor dosimetry used by MIRDcalc is explained in 5.4.2

5.3 OPTIONAL INPUTS

MIRDcalc has several optional inputs that the user may choose to use to for accompanying calculations or output formatting..

5.3.1 (optional) Subject ID

The ***Subject ID*** field is used to associate a name to the entered case data. The ID information entered here will propagate to all output files and output filenames.

5.3.2 (optional) Estimated TIAC uncertainty

Users have the option to enter associated TIAC uncertainties with their biodistribution. This can be entered on a per organ basis, and/or assigned globally.

A full explanation of the uncertainty handling in MIRDcalc can be round in section 6.1.

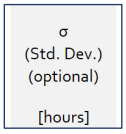

5.3.3 (optional) Modify mass of target organs and the entered mass uncertainty

It is recognized that specific subject organ masses may not match those from the standard phantoms, and this will cause an error in organ dose estimation. A first order approximation for correcting for these differences was presented in MIRD Pamphlet No. 11, and is implemented in MIRDcalc (Snyder et al. 1975). Specifically, it was recommended that the impact of differences in non-reference organ sizes can be accounted for through scaling the self-dose by the ratio of the organ masses to a constant power. The value of the power was set to −2/3 for photon self-dose scaling and −1 for electron and alpha self-dose scaling. Estimations of cross-dose contributions are unchanged when using user-modified organ masses.

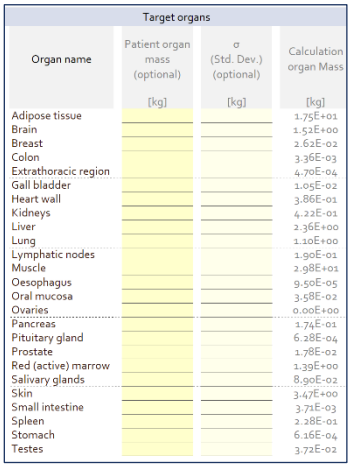

The option to add associated uncertainty to the user-modified mass is also available. This will only impact mass scaling calculations and therefore are only relevant for organs that have had their mass changed.

5.3.4 (optional) Modify *Organ model (S value) uncertainty*

This field can be used to enter a global uncertainty associated with the S values used in the organ level dosimetry. This can be used to account for the uncertainty in the assumption that a specific patient's dosimetry can be modelled using phantom-based organ level methods – it is expected that there will be some difference is patient size/geometry (Mattsson et al. 2015).

Organ model (S value) uncertainty	20%

5.3.5 (optional) Enter Waste TIAC

Users are given the option to enter a "Waste" TIAC. Data in this field will have no effect on the dose calculations. This field is provided to help the users keep track of the amount of activity accounted for.

Hint – double clicking on the "Waste" tag will autocomplete the waste category with all unaccounted-for source activity as prescribed by the theoretical TIAC.

5.4 MIRDCALC OUTPUT

Once case parameters are entered, the user may review input parameters for accuracy

At the top of the output panel, the input dosimetry details are available for the user.

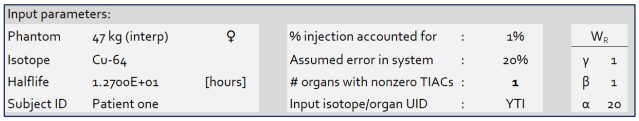

5.4.1 Displayed calculations

The ***Organ Dosimetry Estimates*** are displayed on the interface.

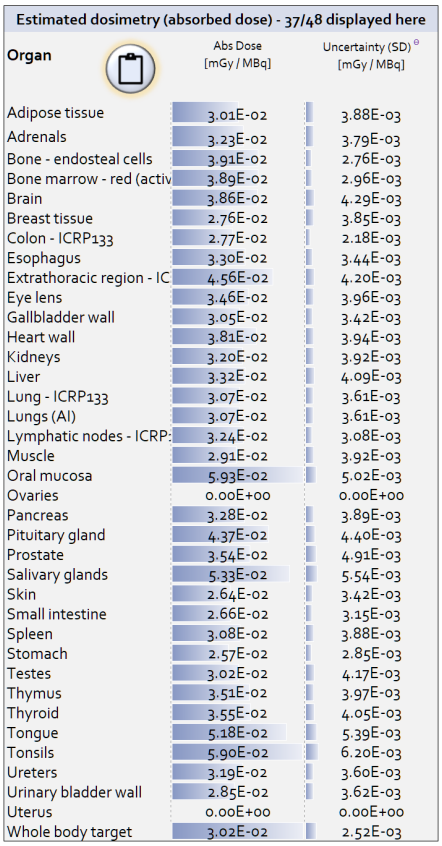

Estimated dosimetry (absorbed dose) - 37/48 displayed here

Organ	Abs Dose [mGy / MBq]	Uncertainty (SD) [mGy / MBq]
Adipose tissue	3.01E-02	3.88E-03
Adrenals	3.23E-02	3.79E-03
Bone - endosteal cells	3.91E-02	2.76E-03
Bone marrow - red (activ	3.89E-02	2.96E-03
Brain	3.86E-02	4.29E-03
Breast tissue	2.76E-02	3.85E-03
Colon - ICRP133	2.77E-02	2.18E-03
Esophagus	3.30E-02	3.44E-03
Extrathoracic region - IC	4.56E-02	4.20E-03
Eye lens	3.46E-02	3.96E-03
Gallbladder wall	3.05E-02	3.42E-03
Heart wall	3.81E-02	3.94E-03
Kidneys	3.20E-02	3.92E-03
Liver	3.32E-02	4.09E-03
Lung - ICRP133	3.07E-02	3.61E-03
Lungs (AI)	3.07E-02	3.61E-03
Lymphatic nodes - ICRP:	3.24E-02	3.08E-03
Muscle	2.91E-02	3.92E-03
Oral mucosa	5.93E-02	5.02E-03
Ovaries	0.00E+00	0.00E+00
Pancreas	3.28E-02	3.89E-03
Pituitary gland	4.37E-02	4.40E-03
Prostate	3.54E-02	4.91E-03
Salivary glands	5.33E-02	5.54E-03
Skin	2.64E-02	3.42E-03
Small intestine	2.66E-02	3.15E-03
Spleen	3.08E-02	3.88E-03
Stomach	2.57E-02	2.85E-03
Testes	3.02E-02	4.17E-03
Thymus	3.51E-02	3.97E-03
Thyroid	3.55E-02	4.05E-03
Tongue	5.18E-02	5.39E-03
Tonsils	5.90E-02	6.20E-03
Ureters	3.19E-02	3.60E-03
Urinary bladder wall	2.85E-02	3.62E-03
Uterus	0.00E+00	0.00E+00
Whole body target	3.02E-02	2.52E-03

5.4.2 Tumor dosimetry

MIRDcalc supports “simplistic” tumor dosimetry. Users may calculate tumor dosimetry by selecting tumor source regions on the organ selection page (see 5.2.4).

MIRDcalc tumor dosimetry is performed by calculating the self dose to a sphere from a given isotope. The user provides the specifications for the sphere volume/composition, as well as the TIAC and isotope to be used for calculation. Dosimetry calculations are based off S values provided by Olguin et. al. (Olguin et al. 2020). Tumor dosimetry is based upon S value interpolation/extrapolation of published data points for user-specified volumes. Interpolation/extrapolation is accomplished via log-log fitting using the two closest published sampling points.

Propagation of uncertainty in tumor dosimetry calculations are derived from user entered uncertainty of TIAC and volume values, and is performed as described in equation 67 of Gear et. al. (Gear et al. 2018)

All MIRDcalc tumor dose calculations are performed independently from organ dosimetry calculations. Cross-dose between tumors and all organs is not considered.

Tumor dosimetry is reported alongside organ dosimetry.

When a MIRDcalc case file is saved, the full isotope/sphere S-value data is included in the save file by default.

5.4.3 Summary dose quantities

Summary dose quantities and associated uncertainties are provided to user in two forms: ***detriment weighted dose (E_{DW})*** and ***effective dose (E)***, displayed in top right of interface.

Detriment Weighted & Effective Dose	[mSv / MBq]	σ [mSv / MBq]
EDW Detr Weight	**2.18E+00**	**9.20E-02**
E Effective Dose	**2.10E+00**	**6.29E-02**

5.4.4 *Detriment weighted dose* (E_{DW})

The *detriment weighed dose* (E_{DW}) is a risk related weighted sum of organ doses. It is calculated using radiation weighting factors and tissue weighting factors described in ICRP 103 (Wrixon 2008). The *detriment weighted dose* is specific to the phantom model used for dose calculations (single sex, potentially modified organ masses).

A greater description of the *detriment weighed dose* can be found in literature (Kofler et al. 2019)

5.4.5 *Effective dose* (E)

The *effective dose* (E) is a risk related weighted sum of organ doses. It is calculated using radiation weighting factors and tissue weighting factors described in ICRP 103 (Wrixon 2008). E is specific to the ICRP phantom model (sex averaged).

5.4.6 Expected dose per injection calculator

In addition, a quick dosimetry calculator/chart is provided. User may enter an administration activity in the activity box (must be in units of MBq), and the dose/injection chart is automatically updated

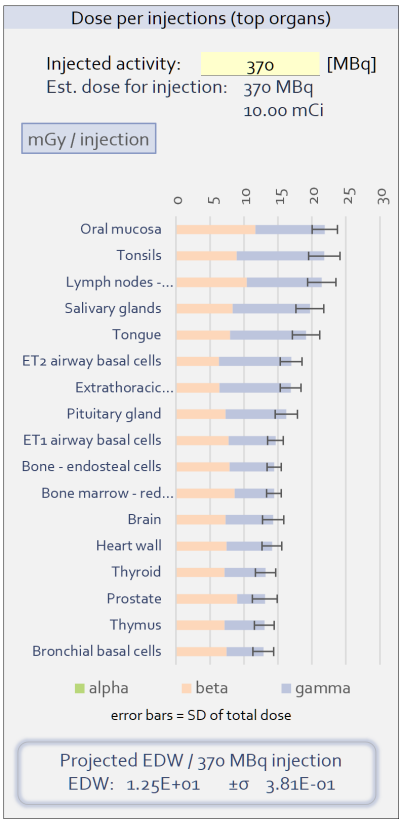

5.4.7 Saving dosimetry calculations

There are two ways to select or save the dosimetry output:

1. User may copy the dosimetry data to the clipboard by clicking the copy button  . One copied, the user may paste the tab delimited data in an external document (e.g. notepad, excel, word…).
2. The user may click the save button 

. This creates a comma delimited MIRDcalc save file automatically saved to "C:\MIRDsoft\MIRDcalc\MIRDcalc_v1.0\MIRDcalc_output \". This file can be reviewed by user and has a more robust accounting of input/output of case. This file can also be used to reload case at a later time (see section 6.4). In addition, clicking the save button will generate a pdf screenshot saved in the same location.

5.5 INTERFACE MAP

The full input/output interface is displayed to the user in a single screen. A screenshot with numbered info-points is displayed below along with a tabulated description (*vide infra*):

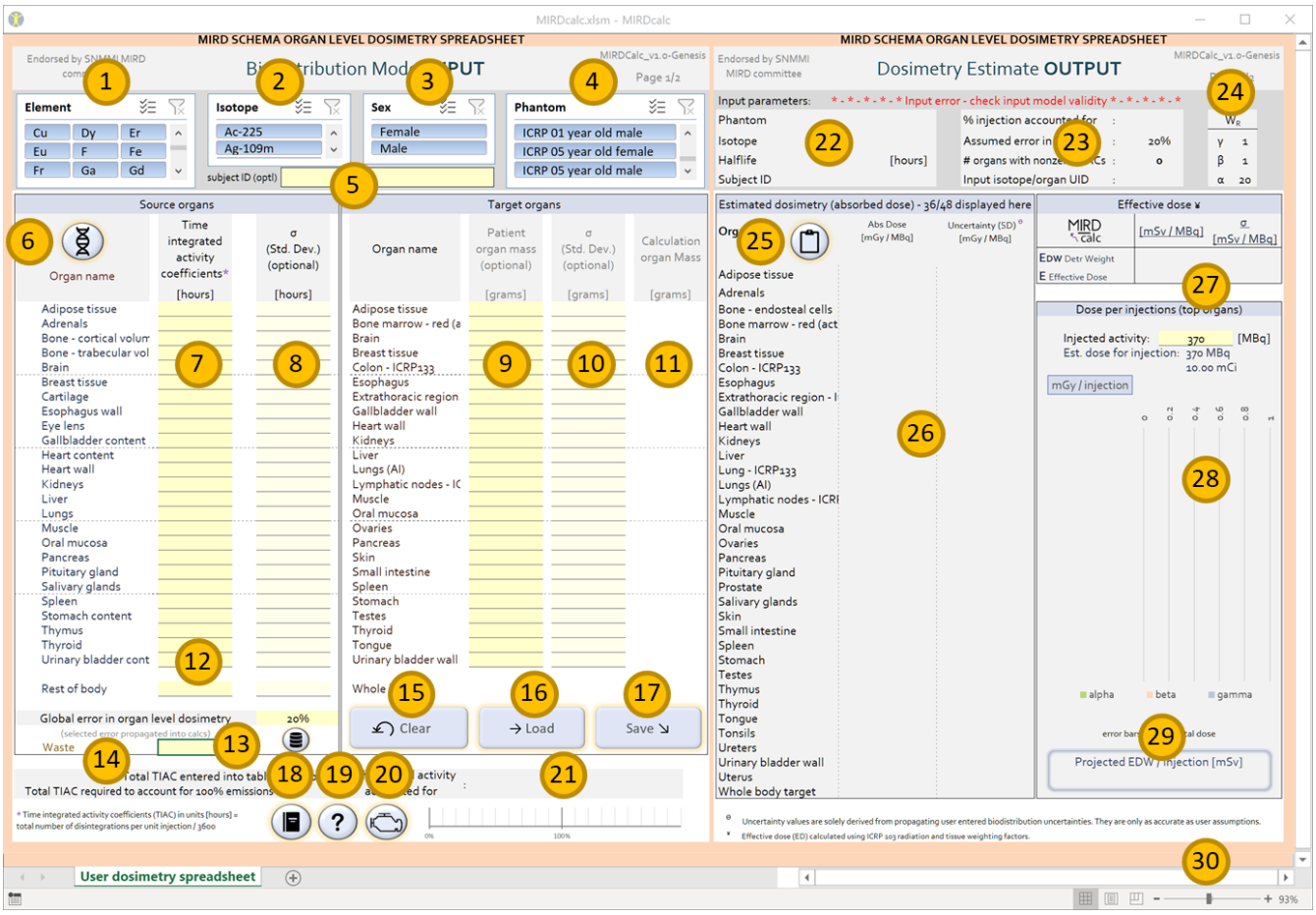

Description of Info-points

1	INPUT SECTION – user selects element to narrow list of isotopes.	2	INPUT SECTION – user selects isotope desired for dosimetric analysis.
3	INPUT SECTION – User selects Male/Female phantom library.	4	INPUT SECTION – user selects phantom, either mass interpolation phantom or ICRP phantom. The mass interpolation phantoms linearly scale the organ masses and S values (used in calculation) between the nearest ICRP phantoms.
5	Subject ID – this is an optional field. Any ID entered will be saved with output.	6	Organ selection button . User may click this button to change the input organs displayed (worksheet allows for 25/79 organs to be displayed and used as input)
7	Time integrated activity coefficient (TIAC) fields - Here is where the user enters the isotope biodistribution in the form of TIACs per organ. Fill all fields for which the user has data. Units are hours.	8	σ (TIAC standard deviation) – User may enter a TIAC uncertainty (standard deviation) for any TIAC. This number is propagated through dose calculations. Units are hours.

9	Patient organ mass fields – The default mass of organs are derived from the phantom used for calculation. The user may choose to change the mass of one or more organs by entering the mass here. This will affect the self-dose of organs (scaling linearly with alpha and beta, and ^2/3 power for gamma) (Snyder et al. 1975). Units must be grams.	10	σ (organ mass standard deviation) – User may enter an organ mass uncertainty (standard deviation) for any mass entered. This number is propagated through the mass adjustment portion of the dose calculation. Units are g.
11	The calculation organ mass column shows the organ masses used in the dosimetry calculations (provides verification for user)	12	Rest of body – This dynamic source region allows user to assign activity in all soft tissues that were not accounted for by other data entries. More information on the MIRDcalc Rest of … regions can be found in section 6.2 of manual.
13	Global error in organ level dosimetry – The user may select a global error is S values to be propagated in all dosimetry calculations. This generally can account for the uncertainties in phantom-based personalized dosimetry. (see error propagation section 6.1)	14	Waste – This field can be used to keep track of activity not entered organs, i.e. activity excreted from patient (sweat, excrement, …). The field can be used to help make sure that 100% of theoretical activity has been accounted for. This data is not used in dose calculations. It is recorded in output dose file.
15	The Clear button can be used to clear the data entered.	16	The Load button can be used load a previously saved file (or a modified saved file). For more information see Case load/save section 6.4.
17	The Save button should be used to save a dosimetry case. When the button is selected, MIRDcalc files are written to C:\MIRDsoft\MIRDcalc\MIRDcalc_output\. For more information see Case load/save section 6.4.	18	The button launches the user manual pdf
19	The button opens the MIRDcalc information page	20	The button opens the dose engine/calculations page. Users may explore this area to better understand software and/or trace calculations.
21	The ***percent theoretical activity accounted for*** meter is a quality assurance graphic that can help the user confirm that their biodistribution is appropriate. The total theoretical TIAC is defined as 100% of the theoretical emissions of a source with unit activity and is equal to the integral of a unit activity curve from 0 to infinity. The total theoretical TIAC can be calculated as $1/\lambda$, or $\ln(2) / \tau_{1/2}$. λ: isotope decay constant $\tau_{1/2}$: isotope half life	22	The ***input parameter*** section displays the user entered parameters used for dose calculation.
23	The input parameter QC panel is displayed to help user confirm intended input correctly entered into system	24	Radiation weighting factors used in *effective dose* calculations (reference: table 2 ICRP 103 (Wrixon 2008)).
25	The button (a) copies the displayed dosimetry calculations to the clipboard and (b) opens a text file showing the copied data.	26	Organ dosimetry, along with uncertainty estimates, for the main target organs are displayed in the dosimetry window, for the user to see. Dosimetry presented here in units of mGy/MBq injected. The uncertainty estimates displayed are purely derived from the uncertainties entered by the user and are only as accurate as the user assumptions. To copy the information in this box, click on the clipboard (#25).
27	*Detriment weighted dose* (E_{DW}) and *Effective dose* (ED) and associated error for selected phantom (top row) and	28	Dose chart provides a quick ranking of the highest dose organs, as well as an opportunity to scale dose by a

	Male/Female average, as defined in ICRP 103 (Wrixon 2008). Units are mSv/MBq. See section 5.4.1		particular injection. This is simply an extra display of information to help the user understand the output.
29	Projected detriment weighted dose provides a phantom specific *effective dose* calculation for a patient given the entered administration activity.	30	Excel zoom bar allows user to zoom in/out.

5.6 SOURCE-TARGET ORGAN REGIONS

A summary of all source and target regions available for use in MIRDcalc can be found in Appendix B and Appendix C.

The source and target regions are derived from the ICRP phantom reference series (Menzel, Clement, and DeLuca 2009).

In addition to the ICRP 133 defined source/target regions, additional regions have been added to MIRDcalc. These include:

New MIRDcalc source regions:

- Heart content (blood region)
- Major blood vessels (blood region)
- Rest of parenchyma see *"Rest of ___" source regions* section 6.2, page 21
- Rest of blood see *"Rest of ___" source regions* section 6.2, page 21
- Rest of body see *"Rest of ___" source regions* section 6.2, page 21

Target regions:

- Colon - ICRP133 Defined in ICRP 133, table 2.3
- Extrathoracic region - ICRP133 Defined in ICRP 133, table 2.3
- Lung - ICRP133 Defined in ICRP 133, table 2.3
- Lymphatic nodes - ICRP133 Defined in ICRP 133, table 2.3
- Whole body target Mass weighted dose of all MIRDcalc target organs

ICRP 133 reference: (Bolch et al. 2016)

5.6.1 Lung target regions

MIRDcalc provides two lung target regions: "Lungs (AI)" and "Lung - ICRP133". It is suggested that "Lung - ICRP133" be used for stochastic risk considerations (for example effective dose calculations) and "Lungs (AI)", representing alveolar-interstitial tissue, be used for deterministic considerations.

5.7 MIRDCALC S-VALUES

S-values are the mathematical basis for organ level dosimetry calculations in the MIRDcalc software, and are originally described in the MIRD primer (Loevinger, Budinger, and Watson 1988), and described here in Appendix A.

The S-values used in MIRDcalc were calculated primarily using the SAF factors published in ICRP publications 133 and 143, respectively (Bolch et al. 2016; Bolch et al. 2020). It is important to note however, that the MIRDcalc project integrated non-yet published data and generated SAF and S-values for two additional sources – heart content and major blood vessels, as needed by the MIRDcalc dynamic blood model - further descriptions to be forthcoming in future publications.

S-values used in any particular case are accessible to users, present by default in the MIRDcalc save files.

6 ADVANCED FEATURES

6.1 UNCERTAINTY PROPIGATION IN MIRDCALC

The use of uncertainty propagation in MIRDcalc dosimetry calculations is optional. Simply leaving uncertainty input cells blank will default calculations to zero uncertainty (the classical standard).

MIRDcalc includes a propagation of uncertainty feature, allowing the user to incorporate the uncertainty in their input to derive an associated uncertainty of their output. To utilize this feature, the user can enter uncertainty values (standard deviation of metrics) in the designated cells, for all data inputs — TIACs, masses, and global S values. The uncertainties entered are propagated through all biodistribution-to-dose calculations, to provide dosimetry with the associated uncertainty. All covariance is assumed to be zero for error propagation calculations in MIRDcalc, with the exception of the male/female dose averaging portion of the e*ffective dose* calculation, where covariance is assumed to be one.

At the time of MIRDcalc software release (2021), uncertainty propagation is relatively new concept to the field of internal dosimetry, and the field has yet to reach consensus as how to properly utilize this information. MIRDcalc includes this feature in an effort to enable and encourage the field to better grasp our understanding of our data, and its capacities and limitations. It should be understood by the user that **all uncertainty estimates presented by MIRDcalc are reflective of user entered uncertainty values propagated through calculations and are only as accurate as the user's data and assumptions**. MIRDcalc performs no inherent uncertainty estimation.

6.2 MIRDCALC "REST OF ___" SOURCE REGIONS

The MIRDcalc software has three ***dynamic*** source regions –

MIRDcalc "Rest of ___" source regions
Rest of body
Rest of blood
Rest of parenchyma

TIACs entered into the *Rest of* regions get distributed, weighted by mass, into all *unaccounted-for* source organ regions. *Unaccounted-for* source regions are defined as the non-overlapping source regions for which the user has not explicitly assigned TIACs to. The *Rest of* regions are dynamic – as a user enters/assigns TIAC values to source organs, the make-up and total mass of the *Rest of* regions adjust accordingly.

This strategy is modelled after the "additive approach" for handling *other tissues* presented in ICRP Publication 133, equation 2.10 (Bolch et al. 2016). Technically MIRDcalc does not update specific absorbed fractions (SAFs) values as described in the report, but instead (perhaps more simply) distributes

the dynamic TIAC into non-defined organs. The two processes are mathematically equivalent with respect to dose calculations.

The subregions that make up each of the MIRDcalc defined *Rest of* regions are shown in Appendix D. An example case outlining *Rest of* TIAC distribution is shown in Appendix E. Users may find the detailed distribution of Rest of ___ region TIACs in Section D of any case save file.

6.3 MIRDCALC BLOOD SOURCE MODEL

Separating blood and other (soft/hard) tissues poses a challenge for dosimetry models, as they can occupy the same space (within the model) but have separate tracer kinetics. While the classic strategy is to collapse the blood into a *rest-of-body* or *remainder* or *blood* term, MIRDcalc handles the overlap differently.

In the MIRDcalc model, any TIAC entered for an organ/region defines the blood *and* parenchyma source emissions from that organ/region – this allows for the easy use of imaging-derived input. MIRDcalc keeps track of the separate blood and parenchyma masses accounted for in the regions of user entered TIACs, and removes them from the *Rest of body*, *Rest of blood*, and *Rest of parenchyma* input terms, which are described in section 6.2. These "*Rest of __*" terms can then be used to distribute emission sources in unaccounted for tissues.

Users may account for the blood and soft tissue remainder TIACs using the following sources:

- Organ regions (defining blood and parenchyma)
- Blood regions - *Heart content* and *Major blood vessels*
- The *Rest of body* source region – distributes to all unaccounted-for blood and soft/hard tissues
- Separate *Rest of blood* and *Rest of parenchyma* source regions, which separately distribute to the blood and parenchyma, respectively.

The choice of which regions to use depends on the users' measuring methods and assumptions. For example, if the user is defining the remainder (unaccounted for activity) from imaging, they may prefer to use a background measurement derived from imaging, accounting for both remainder blood and parenchyma, and assign the measured TIAC to the *Rest of body* source region, which distributes the source activity across the blood and parenchyma. Alternatively, if the user has specific blood measurements – from blood samples or blood pool imaging - they may separate the blood and parenchyma input, using the blood measurements for the *Rest of blood* source region and alternative estimates for the *Rest of parenchyma* source region.

Ultimately, the methods and assumptions used to derive the biodistribution input, including blood, are entirely up to the user. MIRDcalc is designed to give users' options as to how to characterize the input biodistribution.

6.4 CASE LOAD/SAVE

To estimate dosimetry in MIRDcalc, the user needs to load or input case parameters (element/isotope, phantom, biodistribution TIACs). This information can be entered manually on the graphical user interface or loaded with a MIRDcalc input file.

MIRDcalc input files: MIRDcalc input files are text files that can be stored locally and used to load specific input parameters into the MIRDcalc spreadsheet. The required format of input files is exemplified in any/all saved output files (under CASE LOADING BLOCK). To manually create a MIRDcalc input file, we suggest starting with a MIRDcalc save file, and editing the filename/data as desired.

MIRDcalc output files: When a case is properly loaded the user can click the save button 

to archive case. This creates a comma delimited MIRDcalc save file automatically saved to the default "C:\MIRDsoft\MIRDcalc\MIRDcalc_v1.0\MIRDcalc_output\". MIRDcalc save files are in .csv format and can be viewed with a text editor (e.g. notepad). The MIRDcalc save files include by default a CASE LOADING BLOCK and therefore can be used to reload the saved case.

6.5 COMMAND LINE AND BATCH PROCESSING

MIRDcalc supports two methods of running dosimetry calculations: via user interface or via spool processing. The command line/batch processing feature allows MIRDcalc dose calculations to run without an interface nor user interaction and allows for the batch processing of populations of data.

To use the batch processing feature:

1. Place MIRDcalc case file(s) in the spool folder ("C:\MIRDsoft\MIRDcalc\MIRDcalc_v1.0\MIRDcalc_spool\")

2. Launch MIRDcalc.

   When MIRDcalc is launched, the program first checks the spool folder for MIRDcalc load files – if MIRDcalc load files are found, MIRDcalc will run in batch mode – dosimetry output files will be automatically generated for each input file, the input file will be deleted, and the program will close.

Note- if the user wants to run MIRDcalc with the graphical user interface, they need to ensure that the spool folder is empty.

6.6 PHANTOM INTERPOLATION FOR KG-DEFINED PHANTOMS

The user may use a selection of phantom models for dose calculations. These include the ICRP phantom series (Male/Female: Newborn, 1 year old, 5 year old, 10 year old, 15 year old and Adult). In addition, the user may select from the phantom list a phantom model based on weight. Selection of a weight-based phantom will load a linearly interpolated phantom model from the two closest-by-mass phantoms in the ICRP phantom series. Specifically, the phantom organ masses and S values will be linearly scaled using

the selected mass relative to the phantom model masses. A description of scaled mass-defined phantoms is shown in Appendix F.

6.7 PREPARED ICRP 128 CASE LOAD FILES

The MIRDcalc distribution comes with formatted biodistribution case load files for the 580 ICRP 128 tracers.

The International Commission on Radiological Protection (ICRP) have promulgated reference biokinetic data, in the form of time-integrated activity coefficients, for a number of radiopharmaceuticals in common use (ICRP Publication 128) (Mattsson et al. 2015). The reference TIACs provided in ICRP 128 have been assimilated into a database of comma-separated text (*.csv) files, formatted properly for direct import into MIRDcalc; these case files are provided with the MIRDcalc v1.0-Genesis distribution, and may be accessed and loaded using by clicking the *Database* button in the MIRDcalc GUI  .

The reference case source files can be found in the "C:\MIRDsoft\MIRDcalc\MIRDcalc_v1.0\Lib\MCNM_reference_cases\" directory. The filenames have the following naming convention: "*<radionuclide> _ <radiopharmaceutical name> for <phantom name>.csv*".

Importantly, upon loading a reference case file, MIRDcalc will immediately compute reference dose coefficients – the appropriate radionuclide and phantom will be automatically selected. However, the user should keep in mind that further modification of any setting (e.g. phantom, radionuclide, TIAC, organ masses) will affect a departure from *reference* dosimetry.

As a critical note, the reference TIACs of ICRP 128 were intended to be used for dosimetry calculations in the previous generation stylized anthropomorphic phantom series. Certain assumptions/modifications were made in utilizing these TIACs in current-generation ICRP reference phantoms:

- The upper large intestine (ULI) and lower large intestine (LLI) regions of the GI tract have been adjusted in the current-generation reference phantoms to instead consist of the right colon, left colon, and rectosigmoid colon regions. TIACs associated with the ULI and LLI wall and contents regions were re-apportioned to the left/right/rectosigmoid colon regions using the following formulae (Andersson et al. 2014):

$$\tilde{a}\left(r_{Right\ colon}, T_D\right) = 0.71 \cdot \tilde{a}(r_{ULI}, T_D)$$
$$\tilde{a}\left(r_{Left\ colon}, T_D\right) = 0.29 \cdot \tilde{a}(r_{ULI}, T_D) + 0.56 \cdot \tilde{a}(r_{LLI}, T_D)$$
$$\tilde{a}\left(r_{Rectosigmoid\ colon}, T_D\right) = 0.44 \cdot \tilde{a}(r_{LLI}, T_D)$$
$$\tilde{a}\left(r_{Right\ colon\ contents}, T_D\right) = 0.71\ \tilde{a}(r_{ULI\ contents}, T_D)$$
$$\tilde{a}\left(r_{Left\ colon\ contents}, T_D\right) = 0.29\ \tilde{a}(r_{ULI\ contents}, T_D) + 0.74\ \tilde{a}(r_{LLI\ contents}, T_D)$$
$$\tilde{a}\left(r_{Rectosigmoid\ colon\ contents}, T_D\right) = 0.26\ \tilde{a}(r_{LLI\ contents}, T_D)$$

- For TIACs originally assigned to 'cortical bone' or 'trabecular bone', the TIAC was assigned to the corresponding bone volumes for radiopharmaceuticals with effective half-lives longer than 15 days, and to the bone surfaces for radiopharmaceuticals with effective half-lives shorter than 15 days

- For TIACs originally assigned only to 'bone', first the half-life was evaluated as above to determine surface vs. volume localization. Then, the TIAC was apportioned to the cortical bone and trabecular bone using the following cortical:trabecular ratios:

    - 40:60 ratio for bone surface-associated activity for adults, 15 and 10 year old
    - 30:70 ratio for bone surface-associated activity for 5 and 1 year old
    - 80:20 ratio for bone volume-associated activity for adults, 15 and 10 year old
    - 60:40 ratio for bone volume-associated activity for 5 and 1 year old

- TIACs specified for 'blood' in ICRP 128 are assigned to the 'Blood (classic ICRP)' source region in MIRDcalc. In such cases where a blood TIAC is specified, the 'other organs and tissues' TIAC given in ICRP 128 is assigned to the '*Rest of parenchyma*' MIRDcalc source region.

    - If no TIAC is explicitly specified for the blood in ICRP 128, then the 'other organs and tissues' TIAC is assigned to the '*Rest of body*' MIRDcalc source region

6.8 RISK INDEX

MIRDcalc provides a calculation of *Risk Index* (RI), found in the output of a case save file. This value is presently used for research and has not been established for use in the field.

Consideration of medical exposures is important for low levels of radiation absorbed doses. When exposure to ionizing radiation occurs, it is essential to be able evaluate how much radiation a patient receives, and to be able to it in context of risk and benefit. Having accurate metrics and quantities to understand those variables is critical in the process of justification and optimization in medical imaging.

Traditionally the *effective dose* has been used as a risk indicator, and as a value for comparison in medical radiation procedures, even though this application for medical imaging was not the original intended use of this radiation protection quantity. It has been proposed that the risk determination process for medical diagnostic use of ionizing radiation can be adjusted using newer data, more specific modeling, and presented in more refined terms. Using appropriate risk values for the individual tissues at risk, and stratification by age and sex may offer greater insight into understanding individual risk. For this reason, the RI value has been proposed in literature.

The RI is a special and advanced feature included in MIRDcalc, the aim of this quantity is to provide to specialized users a more clinically relevant alternative to the *effective dose* for risk assessment and optimization processes for the use of radiopharmaceuticals in nuclear medicine. The RI is recently established in the literature (O'Reilly et al. 2016; Brown et al. 2020) and has been integrated as an output calculation in the MIRDcalc software.

The RI estimation is defined as a ratio of the estimated added risk of cancer from specific radiation exposure, relative to the estimated natural risk of cancer. For implementation, we estimated the lifetime attributable risk of cancer (LAR) from a given exposure using the National Cancer Institute's Radiation

Risk Assessment Tool (RadRAT) (Berrington de Gonzalez et al. 2012). The baseline, the natural incidence of cancer in a population with an absence of exposure, was derived from the SEER database as defined in RadRAT. All risks are extracted on an age and sex basis.

$$Risk\ Index = \frac{\text{Estimate Radiation Induced Cancer Risk}}{\text{Natural Incidence of Cancer}}\ x\ 100$$

Several reports like BEIR VII, EPA, NCI, ICRP provide data and methodologies in order to estimate LAR values from radiation exposure for age, sex. LAR values can be calculated for incidence or mortality of cancer as well for specific organs/tissue cancer sites and for the addition of all types of cancer.

In MIRDcalc age and sex specific LAR values are estimated from organ absorbed doses using the approach of the NCI for cancer incidence, LAR for specific organs is calculated and summed to obtain the total whole-body LAR.

As an example, a RI of 1.0 would suggest a patient has a 1% higher chance of radiation induced cancer when compared to their natural probability of cancer incidence. Note that the percentage is over the baseline natural risk of cancer.

The user should be aware that the values of LAR are based on the LNT model and that the numerical values are inferences of the extrapolation of that model to low absorbed doses. Numerous publications point out that this model is not suitable for calculating individual risk at low doses. It is therefore not advisable to attribute a LAR or RI value as a risk assessment to any one individual patient.

Ultimately, the RI is presented in MIRDcalc as a resource for users. The field has yet to come to consensus on its appropriate use. This will likely be in areas of optimization and comparative risk assessments. The RI presents a newly designed variable to help understand and communicate risk associated with diagnostic radiation doses, and can potentially be used as a substitute or complementary measurement of the ED.

Values of LAR ([(case / 100k) /MBq]) and RI (%/MBq) are provided for ages 0, 5, 10, 15, 20, 30, 40, 50, 60, 70, 80, 90, 100 years old. From the output the user can select the proximal age between the available data ages and then perform the interpolation for the desired age. For pediatric patients the user may run MIRDcalc for the two close ages and then perform the interpolation.

For traceability of the RI, values used for calculation of LAR and the natural risk of cancer in MIRDcalc are provided in the following tables. Estimates of Lifetime risk of radiation-related cancer are provided in tables Table 1 and Table 2 for males and females respectively, values are applicable for a particular age of exposure and for a single-acute absorbed dose of 0.1 Gy. Estimates of cancer incidence are shown for several site-specific solid cancers, leukemia, and all types of cancers. Table 3 and Table 4 shows lifetime risks of cancer incidence in the absence of exposure, i.e., the natural Incidence of cancer by age and sex per 100,000 population.

Example use of MIRDcalc RI can be found in Appendix G.

Table 1- Lifetime Attributable Risk of Cancer Incidence by age and site for males (Number of cases per 100,000 persons exposed to a single dose of 0.1 Gy). Derived from RadRAT 4.2.

Cancer Site/Age	0	5	10	15	20	30	40	50	60	70	80
Oral Cavity & Pharynx	83.7	70.3	58.5	48.7	40.6	27.9	24.6	18.4	11.1	5.12	1.61
Esophagus	102	86.5	72.9	61.4	51.8	36.7	35	30	21.3	11.2	3.8
Stomach	256	212	174	142	117	76.8	71.5	62.2	47.7	29.3	12.1
Colon	523	447	379	321	273	195	187	167	129	74.5	26.3
Rectum	52.7	45	38	32.1	27.2	19.1	17.8	14.9	10.4	5.48	1.88
Liver	167	139	115	95	78.8	53.9	51.4	44.3	34.3	21.5	9.49
Gallbladder	0	0	0	0	0	0	0	0	0	0	0
Pancreas	89.1	76.2	64.6	54.8	46.6	33.5	32.2	28.4	21.1	11.7	3.95
Lung	511	428	355	295	246	172	170	159	131	84.2	37.8
Prostate	307	266	229	197	170	128	127	115	75.4	30.3	7.85
Bladder	372	319	271	230	196	142	140	132	108	67.2	26.4
Kidney	122	104	88.8	75.8	64.8	46.6	43	35.5	23.6	11.3	3.31
Nervous System	152	104	79.5	63.1	50.6	32.6	27.6	21.4	14	6.35	1.64
Thyroid	296	197	130	85	55.4	22.6	8.59	3	0.88	0.184	0.0243
Other	1020	851	701	569	460	298	259	212	150	80.5	26.7
Leukemia	364	177	136	115	103	91.5	91.5	94.3	99	95.6	69.5
All cancers	4418	3522	2892	2385	1981	1376	1286	1137	877	534	232

Table 2: Lifetime Attributable Risk of Cancer Incidence by age and site for females (Number of cases per 100,000 persons exposed to a single dose of 0.1 Gy). Derived from RadRAT 4.2.

Cancer Site/Age	0	5	10	15	20	30	40	50	60	70	80
Oral Cavity & Pharynx	83.7	70.2	58.5	48.6	40.2	27.2	24.2	19.5	13.6	7.25	2.53
Esophagus	42.4	36.3	30.9	26.3	22.4	16.1	15.5	14	10.7	6.15	2.35
Stomach	307	254	208	171	139	91.6	85.6	75.5	60.1	39.3	17.7
Colon	350	299	254	215	182	130	124	112	89.9	57.7	23
Rectum	48.2	40.9	34.4	28.9	24.3	16.8	15.5	13.1	9.77	5.86	2.36
Liver	95.4	78.8	64.8	53.3	43.9	29.6	28.6	26.1	21.5	14.5	6.89
Gallbladder	0	0	0	0	0	0	0	0	0	0	0
Pancreas	89.9	76.6	64.9	55	46.6	33.2	32	29	23	14.3	5.65
Lung	1210	1020	849	711	596	418	408	378	303	190	86.9
Breast	1810	1420	1100	857	663	386	209	101	43	15.2	3.76
Ovary	164	138	115	95.5	79.6	54.6	48.8	39.1	27	15.1	5.54
Uterus	93.4	78	64.8	53.6	44	28.7	25.9	21.4	15.4	9.25	3.95
Bladder	365	313	266	226	193	139	136	125	102	65.4	27.5
Kidney	79.6	66.7	56.5	47.8	40.4	28.4	26.1	21.9	15.6	8.25	2.76
Nervous System	42.9	28.6	21.6	17	13.5	8.58	7.3	5.76	3.9	1.94	0.585
Thyroid	1650	1100	720	468	298	112	37.8	11.5	3.08	0.63	0.0851
Other	622	515	424	347	281	181	152	119	83	45.8	16.5
Leukemia	329	148	105	88.9	81.1	71.6	72.3	74.1	76.1	73.3	55.4
All cancers	7383	5683	4437	3510	2788	1772	1449	1186	901	570	263

Table 3: Baseline Lifetime Risk estimates of cancer incidence for males, number of cases per 100,000 persons in the absence of exposure – SEER data base (RadRAT 4.2).

Cancer Site/Age	0	5	10	15	20	30	40	50	60	70	80	90	100
Oral Cavity & Pharynx	1430	1440	1440	1440	1450	1460	1460	1380	1140	795	478	269	153
Esophagus	757	764	765	766	770	779	789	789	727	570	351	184	105
Stomach	1100	1110	1110	1110	1110	1120	1130	1120	1080	941	695	395	225
Colon	4080	4120	4120	4120	4140	4190	4230	4260	4130	3660	2710	1590	903
Rectum	1840	1850	1860	1860	1870	1890	1890	1850	1670	1310	833	458	260
Liver	833	837	837	837	841	849	856	821	681	508	286	147	84
Gallbladder	286	288	288	289	290	294	297	299	295	269	211	126	72
Pancreas	1260	1270	1270	1280	1280	1300	1310	1320	1260	1070	747	414	235
Lung	7930	8000	8010	8020	8060	8160	8290	8410	8200	6800	4030	2010	1140
Prostate	16400	16500	16500	16600	16600	16900	17200	17600	16700	12100	6110	3110	1760
Bladder	3690	3720	3730	3730	3750	3790	3840	3910	3880	3530	2610	1510	856
Kidney	1770	1780	1780	1780	1790	1800	1810	1760	1570	1180	701	359	204
Nervous System	661	646	630	617	609	590	561	518	448	344	195	98	55
Thyroid	376	380	380	379	378	366	332	285	220	138	66	30	17
Other & Ill-defined Sites	4970	4980	4980	4960	4940	4810	4600	4330	3890	3160	2160	1210	685
Leukemia	939	903	883	868	854	837	816	793	759	685	524	307	175
All cancers	48322	48588	48583	48656	48732	49135	49411	49445	46650	37060	22707	12216	6928

Table 4: Baseline Lifetime Risk estimates of cancer incidence for females, number of cases per 100,000 persons in the absence of exposure – SEER data base (RadRAT 4.2).

Cancer Site/Age	0	5	10	15	20	30	40	50	60	70	80	90	100
Oral Cavity & Pharynx	683	688	688	687	687	681	669	635	562	442	284	157	84
Esophagus	247	249	249	249	249	250	252	250	239	201	136	78	42
Stomach	683	688	689	689	690	691	685	670	637	571	433	258	138
Colon	4200	4230	4230	4240	4240	4260	4260	4230	4060	3620	2770	1610	863
Rectum	1460	1470	1470	1480	1480	1480	1470	1410	1260	1020	695	392	210
Liver	349	349	349	349	349	349	349	343	319	257	156	78	42
Gallbladder	369	372	372	372	373	374	375	373	359	312	234	133	71
Pancreas	1300	1310	1310	1310	1310	1320	1320	1320	1280	1120	817	472	253
Lung	6330	6370	6380	6380	6390	6420	6460	6420	6050	4720	2530	1160	621
Breast	13200	13300	13300	13300	13300	13300	13000	11800	9600	6710	3780	1870	999
Ovary	1440	1460	1460	1450	1450	1440	1410	1310	1110	831	519	265	142
Uterus	3240	3270	3270	3270	3280	3250	3100	2830	2260	1460	789	383	205
Bladder	1190	1200	1200	1200	1200	1210	1210	1210	1160	1010	737	419	224
Kidney	1050	1050	1050	1050	1050	1050	1040	1000	891	684	401	194	104
Nervous System	537	522	507	496	487	466	440	407	351	268	157	79	42
Thyroid	1070	1080	1080	1070	1060	964	794	592	398	231	100	45	24
Other	3180	3170	3170	3150	3130	3040	2870	2600	2230	1730	1130	617	331
Leukemia	722	691	673	660	650	634	613	585	543	474	355	208	112
All cancers	41250	41469	41447	41402	41375	41179	40317	37985	33309	25661	16023	8418	4507

Some case examples of RI calculation are provided in Appendix G: examples of Risk Index calculation.

7 ADDITIONAL ITEMS

7.1 SOFTWARE SHORTCUTS

Automatic "waste" TIAC calculation – *double clicking* on the "Waste" tag will autocomplete the waste category with all unaccounted-for source activity as prescribed by the theoretical total TIAC.

Shortcut to output folder – *double clicking* on the MIRDcalc icon ( ) will launch the default MIRDcalc output folder in the windows browser.

7.2 USAGE QUIRKS

MIRDcalc is built using the "." decimal separator. If you're using a (European) decimal, i.e. writing pi as "3,14", the settings will be changed during MIRDcalc use to use the ".", and on closing it will be changed back to the system preference (recorded at MIRDcalc opening).

7.3 OPERATING SYSTEM

Only PCs running Microsoft Windows 7 or later, with Microsoft Office installed are supported.

MIRDcalc is not supported in Mac environments/virtual machines.

7.4 FEEDBACK

MIRDcalc is built as a community tool. We welcome cooperation and interest to make it better.

We are hoping our MIRDcalc tool is useful to users throughout the community. Any and all feedback is welcome and will be taken under consideration for future development. Please email any comments or suggestions to contact@mirdsoft.org.

8 REFERENCES

Andersson, M., L. Johansson, D. Minarik, S. Leide-Svegborn, and S. Mattsson. 2014. 'Effective dose to adult patients from 338 radiopharmaceuticals estimated using ICRP biokinetic data, ICRP/ICRU computational reference phantoms and ICRP 2007 tissue weighting factors', *EJNMMI Phys*, 1: 9.

Berrington de Gonzalez, A., A. Iulian Apostoaei, L. H. Veiga, P. Rajaraman, B. A. Thomas, F. Owen Hoffman, E. Gilbert, and C. Land. 2012. 'RadRAT: a radiation risk assessment tool for lifetime cancer risk projection', *J Radiol Prot*, 32: 205-22.

Bolch, W. E., K. Eckerman, A. Endo, J. G. S. Hunt, D. W. Jokisch, C. H. Kim, K. P. Kim, C. Lee, J. Li, N. Petoussi-Henss, T. Sato, H. Schlattl, Y. S. Yeom, and M. Zankl. 2020. 'ICRP Publication 143: Paediatric Reference Computational Phantoms', *Ann ICRP*, 49: 5-297.

Bolch, W. E., D. Jokisch, M. Zankl, K. F. Eckerman, T. Fell, R. Manger, A. Endo, J. Hunt, K. P. Kim, N. Petoussi-Henss, and Icrp Authors on Behalf of. 2016. 'ICRP Publication 133: The ICRP computational framework for internal dose assessment for reference adults: specific absorbed fractions', *Ann ICRP*, 45: 5-73.

Brown, J. L., B. Sexton-Stallone, Y. Li, E. C. Frey, S. T. Treves, F. H. Fahey, D. Plyku, X. Cao, G. Sgouros, and W. E. Bolch. 2020. 'Body morphometry appropriate computational phantoms for dose and risk optimization in pediatric renal imaging with Tc-99m DMSA and Tc-99m MAG3', *Phys Med Biol*, 65: 235026.

Gear, J. I., M. G. Cox, J. Gustafsson, K. S. Gleisner, I. Murray, G. Glatting, M. Konijnenberg, and G. D. Flux. 2018. 'EANM practical guidance on uncertainty analysis for molecular radiotherapy absorbed dose calculations', *Eur J Nucl Med Mol Imaging*, 45: 2456-74.

Kofler, C., S. Domal, D. Satoh, S. Dewji, K. Eckerman, and W. E. Bolch. 2019. 'Organ and detriment-weighted dose rate coefficients for exposure to radionuclide-contaminated soil considering body morphometries that differ from reference conditions: adults and children', *Radiat Environ Biophys*, 58: 477-92.

Loevinger, Robert, Thomas Francis Budinger, and Evelyn E. Watson. 1988. *MIRD Primer for Absorbed Dose Calculations* (Society of Nuclear Medicine).

Mattsson, S., L. Johansson, S. Leide Svegborn, J. Liniecki, D. Nosske, K. A. Riklund, M. Stabin, D. Taylor, W. Bolch, S. Carlsson, K. Eckerman, A. Giussani, L. Soderberg, S. Valind, and Icrp. 2015. 'ICRP 128 - Radiation Dose to Patients from Radiopharmaceuticals: a Compendium of Current Information Related to Frequently Used Substances', *Ann ICRP*, 44: 7-321.

Menzel, H. G., C. Clement, and P. DeLuca. 2009. 'ICRP Publication 110. Realistic reference phantoms: an ICRP/ICRU joint effort. A report of adult reference computational phantoms', *Ann ICRP*, 39: 1-164.

O'Reilly, S. E., D. Plyku, G. Sgouros, F. H. Fahey, S. Ted Treves, E. C. Frey, and W. E. Bolch. 2016. 'A risk index for pediatric patients undergoing diagnostic imaging with (99m)Tc-dimercaptosuccinic acid that accounts for body habitus', *Phys Med Biol*, 61: 2319-32.

Olguin, E., B. President, M. Ghaly, E. Frey, G. Sgouros, and W. E. Bolch. 2020. 'Specific absorbed fractions and radionuclide S-values for tumors of varying size and composition', *Phys Med Biol*, 65: 235015.

Snyder, WS, MR Ford, GG Warner, and SB Watson. 1975. "MIRD Pamphlet #11: "S," Absorbed Dose per Unit Cumulated Activity for Selected Radionuclides and Organs." In *SNMMI publications*.

Wrixon, A. D. 2008. 'ICRP 103 - The 2007 Recommendations of the International Commission on Radiological Protection', *Journal of Radiological Protection*, 28: 161-68.

APPENDIX A: NUCLEAR MEDICINE PHYSICS – A HANDBOOK FOR TEACHERS AND STUDENTS

IAEA NUCLEAR MEDICINE PHYSICS A HANDBOOK FOR TEACHERS AND STUDENTS

Chapter 18 - INTERNAL DOSIMETRY

Author: Cecilia Hindorf, PhD

Published by the International Atomic Energy Agency, Nuclear Medicine Physics, IAEA, Vienna (2015)

https://www.iaea.org/publications/10368/nuclear-medicine-physics

CHAPTER 18

INTERNAL DOSIMETRY

C. HINDORF
Department of Radiation Physics,
Skåne University Hospital,
Lund, Sweden

18.1. THE MEDICAL INTERNAL RADIATION DOSE FORMALISM

18.1.1. Basic concepts

The Committee on Medical Internal Radiation Dose (MIRD) is a committee within the Society of Nuclear Medicine. The MIRD Committee was formed in 1965 with the mission to standardize internal dosimetry calculations, improve the published emission data for radionuclides and enhance the data on pharmacokinetics for radiopharmaceuticals [18.1]. A unified approach to internal dosimetry was published by the MIRD Committee in 1968, MIRD Pamphlet No. 1 [18.2], which was updated several times thereafter. Currently, the most well known version is the MIRD Primer from 1991 [18.3]. The latest publication on the formalism was published in 2009 in MIRD Pamphlet No. 21 [18.4], which provides a notation meant to bridge the differences in the formalism used by the MIRD Committee and the International Commission on Radiological Protection (ICRP) [18.5]. The formalism presented in MIRD Pamphlet No. 21 [18.4] will be used here, although some references to the quantities and parameters used in the MIRD Primer [18.3] will be made. All symbols, quantities and units are presented in Tables 18.1 and 18.2.

The MIRD formalism gives a framework for the calculation of the absorbed dose to a certain region, called the target region, from activity in a source region. The absorbed dose D is calculated as the product between the time-integrated activity $\tilde{A}$ and the S value:

$$D = \tilde{A} \cdot S \tag{18.1}$$

The International System of Units unit of absorbed dose is the joule per kilogram (J/kg), with the special name gray (Gy) (1 J/kg = 1 Gy).

The time-integrated activity equals the number of decays that take place in a certain source region, with units Bq · s, while the S value denotes the absorbed dose rate per unit activity, expressed in Gy · (Bq · s)$^{-1}$ or as a multiple thereof, for example, in mGy · (MBq · s)$^{-1}$. The time-integrated activity was named the cumulated activity in the MIRD Primer [18.3] and the absorbed dose rate per unit activity was named the absorbed dose per cumulated activity (or the absorbed dose per decay). A source or a target region can be any well defined volume, for example, the whole body, an organ/tissue, a voxel, a cell or a subcellular structure. The source region is denoted r_S and the target region r_T:

$$D(r_T) = \tilde{A}(r_S) \cdot S(r_T \leftarrow r_S) \tag{18.2}$$

The number of decays in the source region, denoted the time-integrated activity, is calculated as the area under the curve that describes the activity as a function of time in the source region after the administration of the radiopharmaceutical ($A(r_S, t)$). The activity in a region as a function of time is commonly determined from consecutive quantitative imaging sessions, but it could also be assessed via direct measurements of the activity on a tissue biopsy, a blood sample or via single probe measurements of the activity in the whole body. Compartmental modelling is a theoretical method that can be used to predict the activity in a source region in which measurements are impossible.

$$\tilde{A}(r_S) = \int A(r_S,t)\, \mathrm{d}t \tag{18.3}$$

The time-integration period T_D, for which the time-integrated activity in the source region is determined, is commonly chosen from the time of administration of the radiopharmaceutical until infinite time, e.g. 0 to ∞ (Eq. (18.4)). However, the integration period should be matched to the biological end point studied in combination with the time period in which the relevant absorbed dose is delivered.

$$\tilde{A}(r_S,T_D) = \int_0^{T_D} A(r_S,t)\, \mathrm{d}t \tag{18.4}$$

The time-integrated activity coefficient $\tilde{a}$ is defined as the time-integrated activity divided by the administered activity A_0, as can be seen in Eq. (18.5), and has the unit of time. The time-integrated activity coefficient was named the 'residence time' in the MIRD Primer [18.3]. Figure 18.1 further demonstrates the

concept. The area under the curve describing the activity as a function of time equals the area for the rectangle ($\int_0^{T_D} A(r_S,t)\,dt = \tilde{a}(r_S)\cdot A_0$) and the time-integrated activity coefficient can be described as an average time that the activity spends in a source region.

$$\tilde{a}(r_S) = \frac{\tilde{A}(r_S)}{A_0} \tag{18.5}$$

The S value is defined according to Eq. (18.6), which includes the energy emitted E, the probability Y for radiation with energy E to be emitted, the absorbed fraction ϕ and the mass of the target region $M(r_T)$. The absorbed fraction is defined as the fraction of the energy emitted from the source region that is absorbed in the target region and equals a value between 0 and 1. The absorbed fraction is dependent on the shape, size and mass of the source and target regions, the distance and type of material between the source and the target regions, the type of radiation emitted from the source and the energy of the radiation:

$$S = \frac{EY\phi}{M(r_T)} \tag{18.6}$$

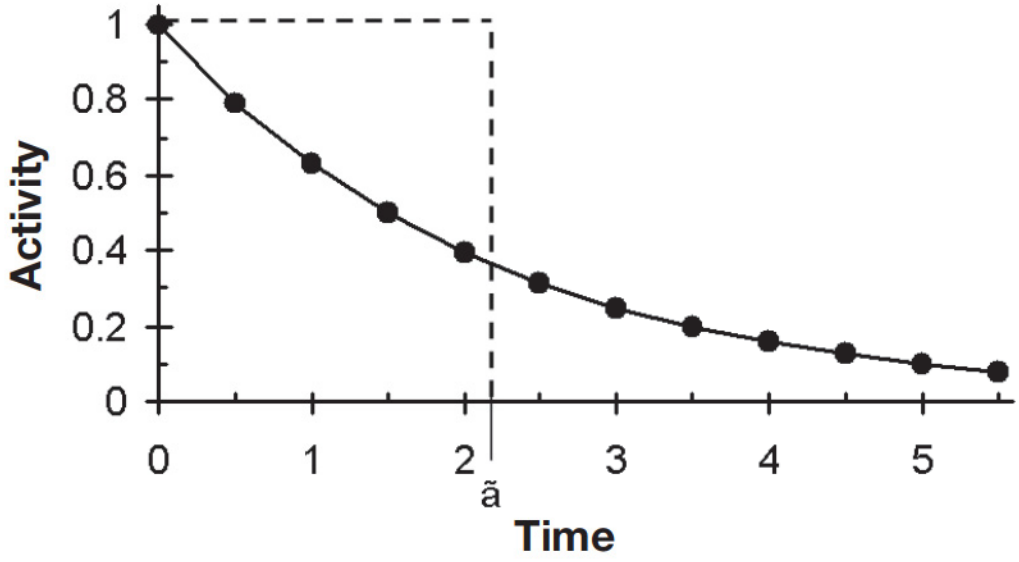

FIG. 18.1. The time-integrated activity coefficient (the residence time in the MIRD Primer [18.3]) is calculated as the time-integrated activity divided by the injected activity, which gives an average time the activity spends in the source region.

The product of the energy emitted E and its probability to be emitted Y is denoted Δ, the mean energy emitted per decay of the radionuclide. The full formalism also includes a summation over all of the transitions i per decay:

$$S(r_T \leftarrow r_S) = \sum_i \frac{\Delta_i \phi(r_T \leftarrow r_S, i)}{M(r_T)} \tag{18.7}$$

The absorbed fraction divided by the mass of the target region is named the specific absorbed fraction Φ:

$$\Phi(r_T \leftarrow r_S, E_i) = \frac{\phi(r_T \leftarrow r_S, E_i)}{M(r_T)} \tag{18.8}$$

The mass of both the source and target regions can vary in time, which means that the absorbed fraction will change as a function of time after the administration, and the full time dependent version of the internal dosimetry nomenclature must be applied (Eq. (18.9)). This phenomenon has been noted in the clinic for tumours, the thyroid and lymph nodes, and can significantly influence the magnitude of the absorbed dose.

$$\Phi(r_T \leftarrow r_S, E_i, t) = \frac{\phi(r_T \leftarrow r_S, E_i, t)}{M(r_T, t)} \tag{18.9}$$

The total mean absorbed dose to the target region $D(r_T)$ is given by summing the separate contributions from each source region r_S (Eq. (18.10)). The self-absorbed dose commonly gives the largest fractional contribution to the total absorbed dose in a target region. The self-absorbed dose refers to when the source and target regions are identical, while the cross-absorbed dose refers to the case in which the source and the target regions are different from each other.

$$D(r_T) = \sum_{r_S} \tilde{A}(r_S) S(r_T \leftarrow r_S) \tag{18.10}$$

The full time dependent version of the MIRD formalism can be found in Eq. (18.11), where $\dot{D}$ denotes the absorbed dose rate:

$$D(r_T, T_D) = \sum_{r_S} \int_0^{T_D} \dot{D}(r_T, t)\, dt = \sum_{r_S} \int_0^{T_D} A(r_S, t) S(r_T \leftarrow r_S, t)\, dt \tag{18.11}$$

TABLE 18.1. EXPLANATION OF SYMBOLS USED IN THE MEDICAL INTERNAL RADIATION DOSE FORMALISM

Symbol	Parameter
R	Type of radiation
r_S	Source region
r_T	Target region
T_D	Integration period

TABLE 18.2. EXPLANATION OF THE SYMBOLS USED TO REPRESENT QUANTITIES IN THE MEDICAL INTERNAL RADIATION DOSE FORMALISM

Symbol	Quantity	Unit
$\tilde{A}(r_S,T_D)$	Time-integrated activity	Bq · s
$\tilde{a}(r_S,T_D)$	Time-integrated activity coefficient	s
$D(r_T)$	Absorbed dose to the target region r_T	Gy
$\dot{D}$	Absorbed dose rate	Gy/s
Δ_i	Mean energy of the ith transition per nuclear transformation	J $(Bq \cdot s)^{-1}$ or MeV $(Bq \cdot s)^{-1}$
E_i	Mean energy of the ith transition	J or MeV
$M(r_T, t)$	Mass of target region	kg
$S(r_T \leftarrow r_S,t)$	Absorbed dose rate per unit activity	mGy $(MBq \cdot s)^{-1}$
t	Time	s
Y_i	Number of ith transitions per nuclear transformation	$(Bq \cdot s)^{-1}$
$\phi(r_T \leftarrow r_S,E_i,t)$	Absorbed fraction	Dimensionless
$\Phi(r_T \leftarrow r_S,E_i,t)$	Specific absorbed fraction	kg^{-1}

18.1.2. The time-integrated activity in the source region

The physical meaning of the time-integrated activity in the source region would be the number of decays in the source region during the relevant time period. The time-integrated activity was named the cumulated activity in the MIRD Primer [18.3].

The activity as a function of time $A(t)$ can often be described by a sum of exponential functions (Eq. (18.12)), where j denotes the number of exponentials, A_j the initial activity for the jth exponential, λ the decay constant for the radionuclide, λ_j the biological decay constant and t the time after the administration of the radiopharmaceutical. The sum of the j coefficients A_j gives the total activity in the source region at the time of administration of the radiopharmaceutical ($t = 0$):

$$A(r_T,t)=\sum_j A_j \cdot e^{-t(\lambda+\lambda_j)} \tag{18.12}$$

The decay constant λ equals the natural logarithm of 2 ($\ln 2 = 0.693$) divided by the half-life. The decay constant in an exponential function matches the slope of the curve it describes (in a linear-log plot of the function).

$$\lambda=\frac{\ln 2}{T_{1/2}} \tag{18.13}$$

The physical half-life $T_{1/2}$ and the biological half-life $T_{1/2,j}$ can be combined into an effective half-life $T_{1/2,\text{eff}}$ according to Eq. (18.14). The effective half-life is always shorter than both the biological and the physical half-lives alone.

$$\frac{1}{T_{1/2,\text{eff}}}=\frac{1}{T_{1/2,j}}+\frac{1}{T_{1/2}} \tag{18.14}$$

The cumulated activity for the relevant time period is commonly calculated as the time integral of an exponential function (Eq. (18.15)). However, other functions could be used, with trapezoidal or Riemann integration (Fig. 18.2). The trapezoidal and the Riemann methods could be reproduced with a higher accuracy than the integration of an exponential, depending on how well the exponential fit could be performed.

$$\tilde{A}=\int_0^\infty A(r_S,0)\, e^{-t(\lambda+\lambda_j)}\, dt=\frac{A(r_S,0)}{\lambda+\lambda_j} \tag{18.15}$$

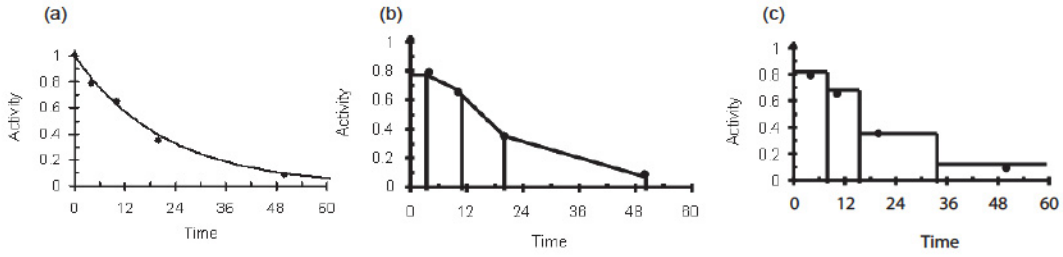

FIG. 18.2. Demonstration of different methods to calculate the time-integrated activity using a fit to an exponential function (a), trapezoidal integration (b) and Riemann integration (c).

Relevant biological data need to be acquired to perform absorbed dose calculations with accuracy. The shape of the fitted curve, which describes the activity as a function of time after the administration of the radiopharmaceutical, can be strongly influenced by the number and timing of the individual activity measurements (see Fig. 18.3). Three data points per exponential phase should be considered the minimum data required to determine the pharmacokinetics, and data points should be followed for at least two to three effective half-lives.

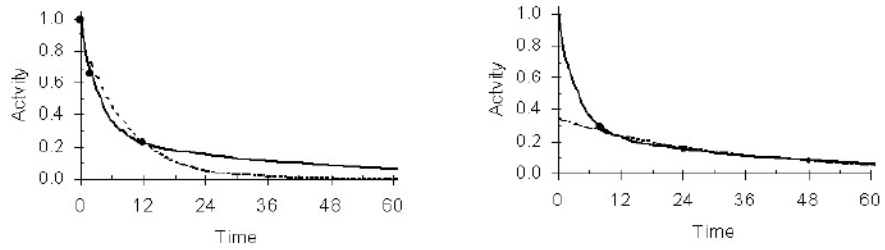

FIG. 18.3. Two examples of the possible influences of curve fitting caused by the number and the timing of activity measurements. The solid line gives the real activity versus time; the dotted line represents the exponential curve fitted to the measurements, which are shown as black dots.

The extrapolation from time zero to the first measurement of the activity in the source region, and the extrapolation from the last measurement of the activity in the source region to infinity, can also strongly influence the accuracy in the time-integrated activity (see Fig. 18.4).

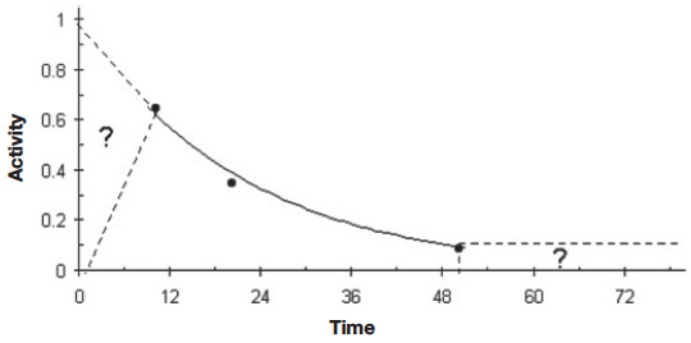

FIG. 18.4. Extrapolation before the first and after the last measurement point.

18.1.3. Absorbed dose rate per unit activity (*S* value)

The *S* value for a certain radionuclide and source–target combination is generated from Monte Carlo simulations in a computer model of the anatomy.

The first models were analytical phantoms, in which the anatomy was described by analytical equations. A coordinate system was introduced and simple geometrical shapes such as spheres or cylinders were placed in the coordinate system to represent important structures of the anatomy. Several analytical phantoms exist: adult man, non-pregnant woman, pregnant woman for each trimester of pregnancy, children (from the newborn and up to 15 years of age) as well as models of the brain, kidneys and unit density spheres.

Voxel based phantoms are the second generation of phantoms used for the calculation of *S* values. These phantoms offer the possibility of more detailed models of the anatomy. Voxel based phantoms can be based on the segmentation of organs from tomographic image data, such as computed tomography (CT) images.

The third generation of phantoms is created using non-uniform rational B-spline (NURBS). NURBS is a mathematical model used in computer graphics to represent surfaces. NURBS provides a method to represent both geometrical shapes and free forms with the same mathematical representation, and the surfaces are flexible and can easily be rotated and translated. This means that movements in time, such as breathing and the cardiac cycle, can be included, allowing for 4-D representations of the phantoms [18.6].

Anatomical phantoms for the calculation of *S* values for use in pre-clinical studies on dogs, rats and mice have also been developed.

A common assumption in radionuclide dosimetry is that radiation emissions can be divided into penetrating (p) or non-penetrating (np) and that the absorbed fractions for these two types can be set to equal 0 and 1, respectively ($\phi_p \approx 0$ and $\phi_{np} \approx 1$). Electrons are often considered non-penetrating and photons

as penetrating radiation, but this is an oversimplification. The validity of the assumption is very dependent on the energy of the radiation in combination with the size of the source region and must, therefore, be assessed on a case by case basis, as is evident from Fig. 18.5. For electrons, the absorbed fraction is greater than 0.9 if the mass of the unit density sphere is greater than 10 g and the electron energy is lower than 1 MeV. This means that the approximation of electrons as non-penetrating radiation is good at an organ level for humans, but as the mass decreases, the approximation ceases to be valid. For photons, the absorbed fraction is less than 0.1 if the mass of the sphere is less than 100 g and if the photon energy is larger than 50 keV. The approximation of considering photons as penetrating radiation is valid in most pre-clinical situations, but as the mass increases, the approximation becomes inappropriate.

The self absorbed S values can be scaled by mass according to the following equation:

$$S(r_T \leftarrow r_T, \text{scaled}) \approx S(r_T \leftarrow r_T, \text{tabulated}) \cdot \frac{M(r_T, \text{tabulated})}{M(r_T, \text{scaled})} \tag{18.16}$$

This is a useful method to adjust the S value found in a table to the true weight of the target region. When scaling an S value, the absorbed fraction is considered to be constant in the interval of scaling. The change in the S value is then set equal to the change in mass of the target. It should be noted that linear interpolation should never be performed in S value tables (Fig. 18.6).

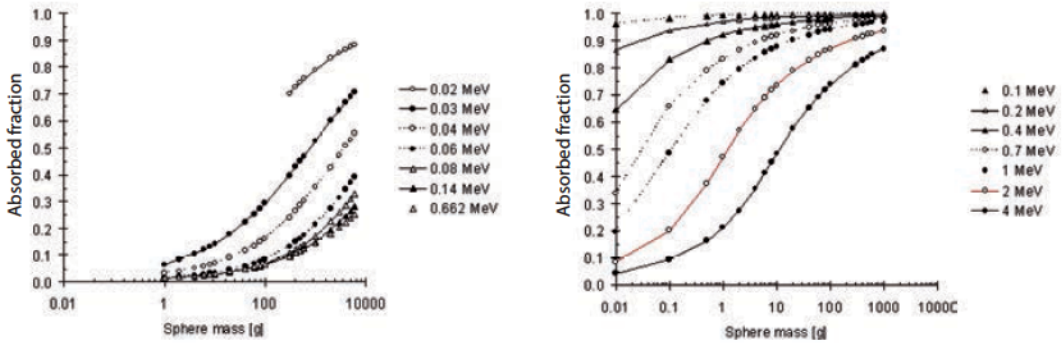

FIG. 18.5. Absorbed fraction for unit density spheres as a function of the mass of the spheres for mono-energetic photons (left) and electrons (right) (data from Ref. [18.7]).

A more sophisticated and probably more accurate way of recalculation of the S value is by separating the total S value into two parts: one for penetrating and one for non-penetrating radiation (S_p and S_{np}, respectively). If the absorbed fraction for non-penetrating radiation is assumed to be equal to 1 ($\phi_{np} = 1$), the S value for penetrating radiation can be calculated (Eqs (18.17)–(18.19)).

The absorbed fractions for photons are relatively constant, so the *S* value for penetrating radiation can be scaled by mass.

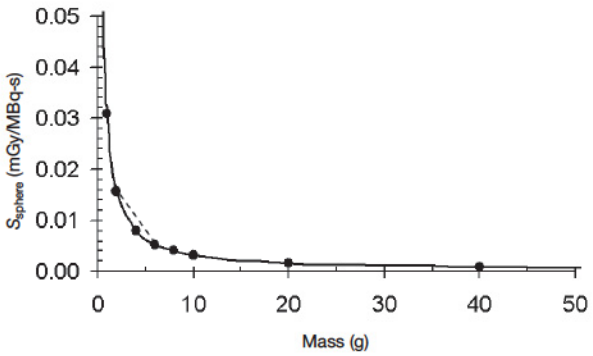

FIG. 18.6. Linear interpolation in S value tables gives S values that are too large. In this particular case for a unit density sphere of ^{131}I, linear scaling would give an S value that is significantly greater than when scaling according to mass is performed.

$$S = S_{\mathrm{p}} + S_{\mathrm{np}} = S_{\mathrm{p}} + \frac{\Delta_{\mathrm{np}}}{m} \tag{18.17}$$

$$S_{\mathrm{p}} = (S - \frac{\Delta_{\mathrm{np}}}{m}) \cdot \frac{m_{\mathrm{phantom}}}{m_{\mathrm{true}}} \tag{18.18}$$

$$S_{\mathrm{recalculated}} = (S - \frac{\Delta_{\mathrm{np}}}{m}) \cdot \frac{m_{\mathrm{phantom}}}{m_{\mathrm{true}}} + \frac{\Delta_{\mathrm{np}}}{m} \tag{18.19}$$

The absorbed fractions for photons and electrons vary according to the initial energy and the volume/mass of the target region and, thus, the suitability of the recalculation will also vary, as was discussed in the previous section (Fig. 18.5).

The principle of reciprocity means that the *S* value is approximately the same for a given combination of source and target regions, i.e. $S(r_T \leftarrow r_S)$ is equal to $S(r_S \leftarrow r_T)$. The reciprocity principle is only truly valid under ideal conditions, in regions with a uniformly distributed radionuclide within a material that is either (i) infinite and homogenous or (ii) absorbs the radiation without scatter. The ideal conditions are not present in the human body, although the reciprocity principle can be seen in *S* value tables for human phantoms as the numbers are almost mirrored along the diagonal axis of the table.

S values for a sphere of a certain volume and material should be scaled according to density if the material in the sphere is different from the material in the phantom (Eq. (18.20)). The technique can be applied when an *S* value for a unit density sphere is used for the calculation of the absorbed dose to a tumour made up of bone or lung. However, it should be noted that an *S* value with the correct mass could be chosen instead of scaling the *S* value for the correct volume by the density.

$$S_{\text{volume, material X}} = S_{\text{volume, material Y}} \cdot \frac{\phi_{\text{material Y}}}{\phi_{\text{material X}}} \tag{18.20}$$

18.1.4. Strengths and limitations inherent in the formalism

Two assumptions are automatically made when the MIRD formalism is applied:

(a) The activity distribution in the source region is assumed to be uniform;
(b) The mean absorbed dose to the target region is calculated.

These assumptions are approximations of the reality. The strengths of the MIRD implementation are its simplicity and ease of use. The limitation of these assumptions is that the absorbed dose may vary throughout the region.

It is important to note that the MIRD formalism does not set any restrictions on either the volume or the shape of the source or target, as long as uniformity can be assumed. This means that the source and target volumes could be defined so that the condition of uniformity is met.

The absorbed dose *D* is defined by the International Commission on Radiation Units and Measurements as the quotient of the mean energy imparted $\mathrm{d}\bar{\varepsilon}$ and the mass d*m* [18.8]:

$$D = \frac{\mathrm{d}\bar{\varepsilon}}{\mathrm{d}m} \tag{18.21}$$

The absorbed dose is defined at a point, but it is determined from the mean specific energy and is, thus, a mean value. This is more obvious from an older definition of absorbed dose, where it is defined as the limit of the mean specific energy as the mass approaches zero [18.9]:

$$D = \lim_{m \to 0} \bar{z} \tag{18.22}$$

The dosimetric quantity that considers stochastic effects and is, thus, not based on mean values, is the specific energy z. The specific energy represents a stochastic distribution of individual energy deposition events ε divided by the mass m in which the energy was deposited [18.10]:

$$z = \frac{\varepsilon}{m} \tag{18.23}$$

The unit of the specific energy is joules per kilogram and its special name is gray. Its relevance is especially important in microdosimetry which is the study of energy deposition spectra within small volumes corresponding to the size of a cell or cell nucleus.

The energy imparted to a given volume is the sum of all energy deposits ε_i in the volume:

$$\varepsilon = \sum_i \varepsilon_i \tag{18.24}$$

The energy deposit is the fundamental quantity that can be used for the definition of all other dosimetric quantities. Each energy deposit is the energy deposited in a single interaction i:

$$\varepsilon_i = \varepsilon_{\text{in}} - \varepsilon_{\text{out}} + Q \tag{18.25}$$

where

ε_{in} is the kinetic energy of the incident ionizing particle;
ε_{out} is the sum of the kinetic energies of all ionizing particles leaving the interaction;

and Q is the change in the rest energies of the nucleus and of all of the particles involved in the interaction.

If the rest energy decreases, Q has a positive value and if the rest energy increases, it has a negative value. The unit of energy imparted and energy deposited is joules or electronvolts. The summation of the energy deposits to receive the energy imparted may be performed for one or more events, which is a term denoting the energy imparted from statistically correlated particles, such as a proton and its secondary electrons.

The absorbed dose is a macroscopic entity that corresponds to the mean value of the specific energy per unit mass, but is defined at a point in space.

When considering an extended volume such as an organ in the body, then for the mean absorbed dose to be a true representation of the absorbed dose to the target volume, either radiation equilibrium or charged particle equilibrium must exist. Radiation equilibrium means that the energy entering the volume must equal the energy leaving the volume for both charged and uncharged radiation. The conditions under which radiation equilibrium are present in a volume containing a distributed radioactive source are [18.11]:

— The radioactive source must be uniformly distributed;
— The atomic composition of the medium must be homogeneous;
— The density of the medium must be homogeneous;
— No electric or magnetic fields may disturb the paths of the charged particle.

Charged particle equilibrium always exists if radiation equilibrium exists. However, charged particle equilibrium can exist even if the conditions for radiation equilibrium are not fulfilled.

If only charged particles are emitted from the radioactive source (as is the case for β emitters such as ^{90}Y and ^{32}P), charged particle equilibrium exists if radiative losses are negligible. Radiative losses increase with increasing electron energy and with an increase in the atomic number of the medium. The maximum β energy for pure β emitters commonly used in nuclear medicine (e.g. ^{90}Y, ^{32}P and ^{89}Sr) is less than 2.5 MeV and the ratio of the radiative stopping power to the total stopping power is 0.018 and 0.028 for skeletal muscle and cortical bone, respectively, for an electron energy of 2.5 MeV. This would imply that the radiative losses can be neglected in internal dosimetry and charged particle equilibrium can be assumed.

If both charged and uncharged particles (photons) are emitted (as is the case with most radionuclides used in nuclear medicine), charged particle equilibrium exists if the interaction of the uncharged particles within the volume is negligible. A negligible number of interactions means that the photon absorbed fraction is low. Photon absorbed fractions as a function of mass can be seen in Fig. 18.5, but it should be pointed out that the relative photon contribution for a radionuclide is also dependent on the energy and the probability of emission of electrons. For example, the photon contribution to the absorbed dose cannot be disregarded for ^{111}In in a 10 g sphere, where the photons contribute 45% to the total *S* value.

18.1.4.1. Non-uniform activity distribution

The activity distribution is seldom completely uniform over the whole tissue. This effect was theoretically investigated on a macroscopic level by Howell et al. [18.12] by introducing activity distributions that varied as a

function of the radius of a sphere. The non-uniformity in the activity distribution can be overcome by redefining the source region into a smaller volume. This is a feasible approach until the activity per unit volume becomes small enough to cause a break-down of both radiation and charged particle equilibrium.

Redistribution of the radioactive atoms over time is responsible for creating non-uniformities of the absorbed dose distribution over time. This effect is handled indirectly in the MIRD formalism, which utilizes the concept of cumulated activity, defined as the total number of decays during the time of integration. However, in most practical applications of MIRD dosimetry, heterogeneities of source distribution within organs are neglected.

18.1.4.2. Non-uniform absorbed dose distribution

If the activity of an α or β emitting radionuclide is uniformly distributed within a sphere, then the absorbed dose distribution will be uniform from the centre of the sphere out to a distance from the rim corresponding to the range of the most energetic particle emission. If the radius of the sphere is large relative to the particle emission ranges, then radiation equilibrium will be established except at the rim and the mean absorbed dose will give a representative value of the absorbed dose. If the radius of the sphere is of the same order as the range of the emitted electrons, significant gradients in the absorbed dose distribution will be formed at the borders of the sphere. As a rule of thumb, it can be assumed that the absorbed dose at the border of the sphere will be half of the absorbed dose at the centre. If the sphere is small compared to the range of the electrons, charged particle equilibrium is never established and the absorbed dose distribution will never be uniform inside the sphere. For α emitting radionuclides, the absorbed dose is uniform for almost all sized spheres, except within 70–90 μm from the rim, corresponding to the α particle range.

Interfaces between media, such as soft tissue/bone or soft tissue/air, will cause non-uniformity in the absorbed dose distribution due to differences in backscatter. This can be significant when estimating the contribution of absorbed dose to the stem cells in the bone marrow from backscatter off the bone surfaces. For planar geometry, the maximum increase in absorbed dose was 9%, as determined by Monte Carlo simulations of ^{90}Y. Experimental measurements with ^{32}P showed a maximal increase of 7%, in close agreement with the theoretical estimates. For a spherical interface with a 0.5 mm radius of curvature, the absorbed dose to the whole sphere showed a maximum increase for 0.5 MeV electrons of as much as 12%.

Non-uniformities in the absorbed dose distribution will also be caused by the cross-absorbed dose, i.e. when one organ is next to another such as lung and heart. In human subjects, the separation between organs is sufficiently great

that the cross-absorbed dose results from penetrating photon radiation only. It is important to note that the cross-organ absorbed dose from high energy β emitters, such as ^{90}Y and ^{32}P, can be significant in preclinical small animal studies used to study radiation toxicity. The importance of the cross-absorbed dose in comparison to the self-absorbed dose strongly depends on both the *S* value and the relative size of the time-integrated activity within the source and the target regions.

The MIRD formalism as such is equally applicable to any well defined source and target region combinations [18.13, 18.14]. Depending on the volume and dimensions of the regions, different types of emitted radiation will be of different importance. To conclude the above discussion, a number of factors causing non-uniformity in the absorbed dose distribution have been identified:

— Edge effects due to lack of radiation equilibrium;
— Lack of radiation equilibrium and charged particle equilibrium in the whole volume (high energy electrons emitted in a small volume);
— Few atoms in the volume, causing a lack of radiation equilibrium and introduction of stochastic effects;
— Temporal non-uniformity due to the kinetics of the radiopharmaceutical;
— Gradients due to hot spots;
— Interfaces between media causing backscatter;
— Spatial non-uniformity in the activity distribution.

18.2. INTERNAL DOSIMETRY IN CLINICAL PRACTICE

18.2.1. Introduction

Internal dosimetry is performed with different purposes, which would require different levels of accuracy in the calculated absorbed dose, depending on the subgroup:

— Dosimetry for diagnostic procedures utilized in nuclear medicine;
— Dosimetry for therapeutic procedures (radionuclide therapy);
— Dosimetry in conjunction with accidental intake of radionuclides.

The dosimetry for a diagnostic procedure is performed to optimize the procedure concerning radiation protection consistent with the requirements of an accurate diagnostic test. This is an optimization of a clinical procedure applicable to all persons. The most relevant would, therefore, be to utilize the mean pharmacokinetics for the radiopharmaceutical for the calculation of the time-integrated activity and *S* values based on a reference man

phantom. The ICRP has published the absorbed dose per injected activity for most radiopharmaceuticals used for diagnostic procedures in the clinic in Publication 53 [18.5], with updates published in Publications 80 and 106 [18.15, 18.16].

The purpose of performing dosimetry for a patient that receives radionuclide therapy is to optimize the treatment so as to achieve the highest possible absorbed dose to the tumour, consistent with absorbed dose limiting toxicities. Thus, individualized treatment planning should be performed that takes into account the patient specific pharmacokinetics and biodistribution of the therapeutic agent.

The procedure to apply after an accidental intake of radionuclides must be decided on a case by case basis. The procedure to apply will depend on the level of activity, which radionuclide, the number of persons involved, whether the dosimetry is performed retrospectively or as a precaution, and whether there is a possibility to perform measurements after the intake.

18.2.2. Dosimetry on an organ level

Dosimetry on an organ level could be performed from activity quantification using either 2-D or 3-D images. Two dimensional images may include whole body scans or spot views covering the regions of interest. Three dimensional single photon emission computed tomography (SPECT) is mostly a limited field of view study that includes only the essential structures of interest. The advantage of 3-D tomographic methods is that they avoid the problems associated with corrections for activity in overlying and underlying tissues (e.g. muscle, gut and bone), and corrections for activity in partly overlapping tissues (e.g. liver and right kidney). Three dimensional positron emission tomography (PET) is emerging as a powerful dosimetric tool because of the greater ease and accuracy of radiotracer quantification with this modality.

S value tables for human phantoms can be found in MIRD Pamphlet No. 11 [18.17], in the OLINDA EXM software [18.18] and on the RADAR web site (www.doseinfo-radar.com). OLINDA/EXM stands for organ level internal dose assessment/exponential modelling, and is a software for the calculation of absorbed dose to different organs in the body. OLINDA includes *S* values for most radionuclides and for ten different human phantoms (adult and children at different ages as well as pregnant and non-pregnant female phantoms). Tumours are not included in the phantoms, although the *S* values for unit density spheres provided in the software could be applied for the calculation of the self-absorbed dose to the tumour. OLINDA also includes a module for biokinetic analysis, allowing the user to fit an exponential equation to the data entered on the activity in an organ at different time points. *S* values can be scaled by mass within

OLINDA, thus allowing for a more patient specific dosimetry to be performed. MIRDOSE [18.19] is the predecessor of OLINDA/EXM.

When calculating the absorbed dose with the MIRD formalism and using tabulated *S* values for a phantom, for example, the reference man, it is assumed that the patient's anatomy is the same as that of the phantom. To employ the MIRD scheme and yet make the dosimetry more patient specific, the *S* values can be scaled to the mass of each patient's target organ. Owing to the inverse relation between the absorbed dose and the mass of the target region, scaling can have a considerable influence on the result. The organ mass can be estimated from CT, magnetic resonance imaging or ultrasound images, provided that the anatomical size equals the functional size (the volume/mass of the organ that is actually physiologically functioning and has an activity uptake).

$$S_{\text{patient}} \approx S_{\text{phantom}} \cdot \frac{m_{\text{phantom}}}{m_{\text{patient}}} \tag{18.26}$$

Since it requires a great deal of work to determine the mass of every organ for each patient, it was suggested that the *S* values might be scaled to the total mass of the patient. This is a more crude method, assuming that the organ size follows the total mass of the body. The lean body weight of the patient should be used to avoid unrealistic values of the organ mass and, thus, the *S* values due to obese or very lean patients.

$$S_{\text{patient}} \approx S_{\text{phantom}} \cdot \frac{m_{\text{TB,phantom}}}{m_{\text{TB,patient}}} \tag{18.27}$$

Tumours are not included in reference man phantoms. However, *S* values could be used for spheres of the correct mass to get an approximation of the self-absorbed dose to the tumour. The drawback with this method is that neither the contribution from the cross-absorbed dose from activity in normal organs to the tumour nor the cross-absorbed dose from activity in the tumour to normal organs can be included in the calculations.

18.2.3. Dosimetry on a voxel level

The activity in an image could be quantified on a voxel level, to display the activity present in each voxel. Images that display the activity distribution at different points in time after injection may be co-registered to each other to allow for an exponential fit on a voxel by voxel basis. A parametric image that gives the time-integrated activity (the total number of decays) on a voxel level

can, thus, be calculated. Parametric images that display the biological half-life for each voxel could also be produced by this technique.

The registration of the images acquired at different points in time after the administration becomes essential for the accuracy that can be achieved in the calculation of the time-integrated activity on a voxel level. Another important factor that determines the accuracy in the time-integrated activity and, thus, in the absorbed dose, is the acquired number of counts per voxel (a random error), the accuracy in the attenuation correction (systematic error) and the calibration factor that translates the number of counts to the activity (random and systematic errors). Multimodality imaging such as SPECT/CT and PET/CT facilitates the interpretation of the images as the CT will provide anatomical landmarks to support the functional images, which could change from one acquisition to the next.

A dose point kernel describes the deposited energy as a function of distance from the site of emission of the radiation. Figure 18.7 displays a dose point kernel for 1 MeV mono-energetic electrons. Convolution of a dose point kernel and the activity distribution from an image acquired at a certain time after the injection gives the absorbed dose rate. Dose point kernels provide a tool for fast calculation of the absorbed dose on a voxel level. However, the main drawback is that a dose point kernel is only valid in a homogenous medium, where it is commonly assumed that the body is uniformly unit density soft tissue.

Monte Carlo simulations that use the activity distribution from a functional image (PET or SPECT) and the density distribution from a CT image avoid the problem of non-uniform media, although full Monte Carlo simulations are time consuming. EGS (electron gamma shower), MCNP (Monte Carlo N-particle transport code), Geant and Penelope are commonly used Monte Carlo codes.

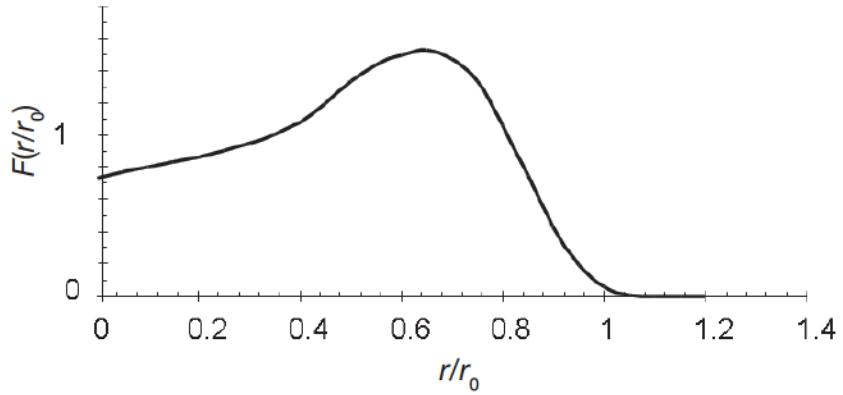

FIG. 18.7. A scaled dose point kernel for 1 MeV electrons [18.20]. r/r_0 expresses the distance scaled to the continuous slowing down approximation range of the electron and $\int_0^\infty F(r/r_0, E_0)\, \mathrm{d}(r/r_0) = 1$.

The concept of dose–volume histograms (DVHs), extensively used to describe the tumour and organ dose distribution in external beam radiotherapy, can be used to display the non-uniformity in the absorbed dose distribution from radionuclide procedures. A differential DVH shows the fraction of the volume that has received a certain absorbed dose as a function of the absorbed dose, while a cumulative DVH shows the fraction of the volume that has received an absorbed dose less than the figure given on the x axis. A truly uniform absorbed dose distribution would produce a differential DVH that shows a single sharp (δ function) peak and a step function on a cumulative DVH. Since the mean absorbed dose in internal dosimetry may be a poor representation of the absorbed dose to the tissue, as discussed above, the use of DVHs might be used to assist the correlation between absorbed dose and biological effect.

REFERENCES

[18.1] STELSON, A.T., WATSON, E.E., CLOUTIER, R.J., A history of medical internal dosimetry, Health Phys. **69** (1995) 766–782.

[18.2] LOEVINGER, R., BERMAN, R.M., A schema for absorbed-dose calculations for biologically-distributed radionuclides, MIRD Pamphlet No. 1, J. Nucl. Med. **9** Suppl. 1 (1968) 7–14.

[18.3] LOEVINGER, R., BUDINGER, T.F., WATSON, E.E., MIRD Primer for Absorbed Dose Calculations (Revised Edition), The Society of Nuclear Medicine, MIRD, Reston, VA (1991).

[18.4] BOLCH, W.E., ECKERMAN, E.F., SGOUROS, G., THOMAS, S.R., A generalized schema for radiopharmaceutical dosimetry — standardization of nomenclature, MIRD Pamphlet No. 21, J. Nucl. Med. **50** (2009) 477–484.

[18.5] INTERNATIONAL COMMISSION ON RADIOLOGICAL PROTECTION, Radiation Dose to Patients from Radiopharmaceuticals, Publication 53, Pergamon Press, Oxford (1987).

[18.6] SEGARS, W.P., TSUI, B.M., FREY, E.C., JOHNSON, G.A., BERR, S.S., Development of a 4-D digital mouse phantom for molecular imaging research, Mol. Imaging Biol. **6** (2004) 149–159.

[18.7] STABIN, M.G., KONIJNENBERG, M.W., Re-evaluation of absorbed fractions for photons and electrons in spheres of various sizes, J. Nucl. Med. **41** (2000) 149–160.

[18.8] INTERNATIONAL COMMISSION ON RADIATION UNITS AND MEASUREMENTS, Fundamental Quantities and Units for Ionizing Radiation, Rep. 60, ICRU, Bethesda, MD (1998).

[18.9] INTERNATIONAL COMMISSION ON RADIATION UNITS AND MEASUREMENTS, Radiation Quantities and Units, Rep. 33, ICRU, Bethesda, MD (1983).

[18.10] INTERNATIONAL COMMISSION ON RADIATION UNITS AND MEASUREMENTS, Microdosimetry, Rep. 36, ICRU, Bethesda, MD (1983).

[18.11] ATTIX, F.H., Introduction to Radiological Physics and Radiation Dosimetry, John Wiley & Sons, New York (1986).

[18.12] HOWELL, R.W., RAO, D.V., SASTRY, K.S.R., Macroscopic dosimetry for radioimmunotherapy: Nonuniform activity distributions in solid tumours, Med. Phys. **16** (1989) 66–74.

[18.13] HOWELL, R.W., The MIRD schema: From organ to cellular dimensions, J. Nucl. Med. **35** (1994) 531–533.

[18.14] KASSIS, I.E., The MIRD approach: Remembering the limitations, J. Nucl. Med. **33** (1992) 781–782.

[18.15] INTERNATIONAL COMMISSION ON RADIOLOGICAL PROTECTION, Radiation Dose to Patients from Radiopharmaceuticals (Addendum to ICRP Publication 53), Publication 80, Pergamon Press, Oxford and New York (1998).

[18.16] INTERNATIONAL COMMISSION ON RADIOLOGICAL PROTECTION, Radiation Dose to Patients from Radiopharmaceuticals (Addendum 3 to ICRP Publication 53), Publication 106, Elsevier (2008).

[18.17] SNYDER, W.S., FORD, M.R., WARNER, G.G., WATSON, S.B., MIRD Pamphlet No. 11, S, Absorbed Dose per Unit Cumulated Activity for Selected Radionuclides and Organs, The Society of Nuclear Medicine, Reston, VA (1975).

[18.18] STABIN, M.G., SPARKS, R.B., CROWE, E., OLINDA/EXM: The second-generation personal computer software for internal dose assessment in nuclear medicine, J. Nucl. Med. **46** (2005) 1023–1027.

[18.19] STABIN, M.G., MIRDOSE: Personal computer software for internal dose assessment in nuclear medicine, J. Nucl. Med. **37** (1996) 538–546.

[18.20] BERGER, M., Improved point kernels for electron and beta-ray dosimetry, NBSIR 73–107, National Bureau of Standards (1973).

APPENDIX B: SUMMARY OF MIRDCALC SOURCE REGIONS

	MIRDcalc	ICRP133	ICRP133
MC order	**MC name**	**Short name**	**Long name**
1	Adipose tissue	Adipose	Adipose
2	Adrenals	Adrenals	Adrenals
3	Alveolar-interstitial (sub lungs)	AI	Alveolar-interstitial
4	Blood (classic ICRP)	Blood	Blood
5	Bone - cortical surface (sub volume)	C-bone-S	Cortical bone surface
6	Bone - cortical volume	C-bone-V	Cortical bone
7	Bone - trabecular surfaces (sub volumes)	T-bone-S	Trabecular bone surface
8	Bone - trabecular volumes	T-bone-V	Trabecular bone
9	Bone marrow - red (active)	R-marrow	Red (active) marrow
10	Bone marrow - yellow (inactive)	Y-marrow	Yellow (inactive) marrow
11	Brain	Brain	Brain
12	Breast tissue	Breast	Breast
13	Bronchial bound region (sub lungs)	Bronchi-b	Bronchial bound region
14	Bronchial sequestered region (sub lungs)	Bronchi-q	Bronchial sequestered region
15	Bronchial surface (sub lungs)	Bronchi	Bronchial surface
16	Bronchiolar bound region (sub lungs)	Brchiole-b	Bronchiolar bound region
17	Bronchiolar sequestered region (sub lungs)	Brchiole-q	Bronchiolar sequestered region
18	Bronchiolar surface (sub lungs)	Brchiole	Bronchiolar surface
19	Cartilage	Cartilage	Cartilage
20	Colon content - left	LC-cont	Left colon content
21	Colon content - rectosigmoid	RS-cont	Rectosigmoid colon content
22	Colon content - right	RC-cont	Right colon content
23	Colon mucosa - left (sub wall)	LC-mucosa	Left colon mucosa
24	Colon mucosa - rectosigmoid (sub wall)	RS-mucosa	Rectosigmoid colon mucosa
25	Colon mucosa - right (sub wall)	RC-mucosa	Right colon mucosa
26	Colon wall - left	LC-wall	Left colon wall
27	Colon wall - rectosigmoid	RS-wall	Rectosigmoid colon wall
28	Colon wall - right	RC-wall	Right colon wall
29	Esophagus - fast (sub wall)	Oesophag-f	Oesophagus - fast
30	Esophagus - slow (sub wall)	Oesophag-s	Oesophagus - slow
31	Esophagus wall	Oesophag-w	Oesophagus
32	ET1 airway surface (sub wall)	ET1-sur	ET1 surface
33	ET1 airway wall	ET1-wall	ET1 wall
34	ET2 airway bound region (sub wall)	ET2-bnd	ET2 bound region
35	ET2 airway sequestered region (sub wall)	ET2-seq	ET2 sequestered region
36	ET2 airway surface (sub wall)	ET2-sur	ET2 surface
37	ET2 airway wall	ET2-wall	ET2 wall
38	Eye lens	Eye-lens	Lens of eye
39	Gallbladder content	GB-cont	Gall bladder content
40	Gallbladder wall	GB-wall	Gall bladder

41	Heart content	-	-
42	Heart wall	Ht-wall	Heart
43	Kidneys	Kidneys	Kidneys
44	Liver	Liver	Liver
45	Lungs	Lungs	Lungs
46	Lymph nodes - extrathoracic	LN-ET	Extrathoracic lymph nodes
47	Lymph nodes - systemic	LN-Sys	Systemic lymph nodes
48	Lymph nodes - thoracic	LN-Th	Thoracic lymph nodes
49	Major blood vessels	-	-
50	Muscle	Muscle	Muscle
51	Oral cavity (gas)	O-cavity	Oral cavity
52	Oral mucosa	O-mucosa	Oral mucosa
53	Ovaries	Ovaries	Ovaries
54	Pancreas	Pancreas	Pancreas
55	Pituitary gland	P-gland	Pituitary gland
56	Prostate	Prostate	Prostate
57	Respiratory tract air (gas)	RT-air	Respiratory tract air
58	Salivary glands	S-glands	Salivary glands
59	Skin	Skin	Skin
60	Small intestine content	SI-cont	Small Intestine contents
61	Small intestine mucosa (sub wall)	SI-mucosa	Small Intestine mucosa
62	Small intestine villi (sub wall)	SI-villi	Small Intestine villi
63	Small intestine wall	SI-wall	Small Intestine wall
64	Spleen	Spleen	Spleen
65	Stomach content	St-cont	Stomach contents
66	Stomach mucosa (sub wall)	St-mucosa	Stomach mucosa
67	Stomach wall	St-wall	Stomach wall
68	Teeth surface (sub volume)	Teeth-S	Teeth surface
69	Teeth volume	Teeth-V	Teeth volume
70	Testes	Testes	Testes
71	Thymus	Thymus	Thymus
72	Thyroid	Thyroid	Thyroid
73	Tongue	Tongue	Tongue
74	Tonsils	Tonsils	Tonsils
75	Ureters	Ureters	Ureters
76	Urinary bladder content	UB-cont	Urinary bladder content
77	Urinary bladder wall	UB-wall	Urinary bladder wall
78	Uterus	Uterus	Uterus
79	Rest of parenchyma (see Appendix D)	-	-
80	Rest of blood (see Appendix D)	-	-
81	Rest of body (see Appendix D)	-	-

APPENDIX C: SUMMARY OF MIRDCALC TARGET REGIONS

	MIRDcalc	ICRP133	ICRP133
MC order	MC name	Short name	Long name
1	Adipose tissue	Adipose	Adipose tissue
2	Adrenals	Adrenals	Adrenals
3	Bone - endosteal cells	Endost-BS	Endosteal cells
4	Bone marrow - red (active)	R-marrow	Red (active) marrow
5	Brain	Brain	Brain
6	Breast tissue	Breast	Breast
7	Bronchial basal cells	Bronch-bas	Bronchi basal cells
8	Bronchial secretory cells	Bronch-sec	Bronchi secretory cells
9	Bronchiolar secretory cells	Bchiol-sec	Bronchiolar secretory cells
10	Colon - ICRP133	-	-
11	Colon - left	LC-stem	Left colon
12	Colon - rectosigmoid	RS-stem	Rectosigmoid Colon
13	Colon - right	RC-stem	Right colon
14	Esophagus	Oesophagus	Oesophagus
15	ET1 airway basal cells	ET1-bas	ET1 basal cells
16	ET2 airway basal cells	ET2-bas	ET2 basal cells
17	Extrathoracic region - ICRP133	-	-
18	Eye lens	Eye-lens	Lens of eye
19	Gallbladder wall	GB-wall	Gall bladder
20	Heart wall	Ht-wall	Heart wall
21	Kidneys	Kidneys	Kidneys
22	Liver	Liver	Liver
23	Lung - ICRP133	-	-
24	Lungs (AI)	AI	Alveolar-interstitial
25	Lymph nodes - extrathoracic	LN-ET	Extrathoracic lymph nodes
26	Lymph nodes - systemic	LN-Sys	Systemic lymph nodes
27	Lymph nodes - thoracic	LN-Th	Thoracic lymph nodes
28	Lymphatic nodes - ICRP133	-	-
29	Muscle	Muscle	Muscle
30	Oral mucosa	O-mucosa	Oral Mucosa
31	Ovaries	Ovaries	Ovaries
32	Pancreas	Pancreas	Pancreas
33	Pituitary gland	P-gland	Pituitary gland
34	Prostate	Prostate	Prostate

35	Salivary glands	S-glands	Salivary glands
36	Skin	Skin	Skin
37	Small intestine	SI-stem	Small intestine
38	Spleen	Spleen	Spleen
39	Stomach	St-stem	Stomach
40	Testes	Testes	Testes
41	Thymus	Thymus	Thymus
42	Thyroid	Thyroid	Thyroid
43	Tongue	Tongue	Tongue
44	Tonsils	Tonsils	Tonsils
45	Ureters	Ureters	Ureters
46	Urinary bladder wall	UB-wall	Urinary bladder
47	Uterus	Uterus	Uterus
48	Whole body target	-	-

APPENDIX D: *REST OF* … REGION DEFINITIONS

MIRDcalc has three *Rest of …* regions that are defined as dynamic mass-weighted combinations of unaccounted-for sub regions. The subregions for each *Rest of …* region is explained below.

REST OF BODY

The dynamic "Rest of body" source term can be used to distribute TIACs to subregions listed below, apportioned by mass. The subregions are only included in the TIAC allotment they have not been defined explicitly by user (see example in Appendix E). The masses used in this dynamic term for relative weighting are the subregion blood and parenchyma masses. The specific masses used in the calculation depend on user-specified phantom selection, and can be reviewed in case save output file. Sex-specific source regions are used only for relevant sex.

Rest of body (dynamic source region based on weighted combination on blood and parenchyma mass)		
Adipose tissue	Gallbladder wall	Salivary glands
Adrenals	Heart content	Skin
Bone - cortical volume	Heart wall	Small intestine wall
Bone - trabecular volumes	Kidneys	Spleen
Bone marrow - red (active)	Liver	Stomach wall
Bone marrow - yellow (inactive)	Lungs	Teeth volume
Brain	Lymph nodes - extrathoracic	Testes
Breast tissue	Lymph nodes - systemic	Thymus
Cartilage	Lymph nodes - thoracic	Thyroid
Colon wall - left	Major blood vessels	Tongue
Colon wall - rectosigmoid	Muscle	Tonsils
Colon wall - right	Oral mucosa	Ureters
Esophagus wall	Ovaries	Urinary bladder wall
ET1 airway wall	Pancreas	Uterus
ET2 airway wall	Pituitary gland	
Eye lens	Prostate	

** The sub regions are only included in Rest of body TIAC distribution if not specifically specified by user.*

REST OF BLOOD

The dynamic "Rest of blood" source term can be used to distribute TIACs to subregions listed below, apportioned by mass. The subregions are only included in the TIAC allotment they have not been defined explicitly by user (see example in Appendix E). The masses used in this dynamic term for relative weighting are the subregion blood masses. The specific masses used in the calculation depend on user-

specified phantom selection, and can be reviewed in case save output file. Sex-specific source regions are used only for relevant sex.

Rest of blood (dynamic source region based on weighted combination on blood mass)		
Cartilage (blood)	Lungs (blood)	Skin (blood)
Colon wall - left (blood)	Lymph nodes - extrathoracic (blood)	Small intestine wall (blood)
Colon wall - rectosigmoid (blood)	Lymph nodes - systemic (blood)	Spleen (blood)
Colon wall - right (blood)	Lymph nodes - thoracic (blood)	Stomach wall (blood)
Esophagus wall (blood)	Major blood vessels (blood)	Testes (blood)
ET1 airway wall (blood)	Muscle (blood)	Thymus (blood)
ET2 airway wall (blood)	Oral mucosa (blood)	Thyroid (blood)
Gallbladder wall (blood)	Ovaries (blood)	Tongue (blood)
Heart content (blood)	Pancreas (blood)	Tonsils (blood)
Heart wall (blood)	Pituitary gland (blood)	Ureters (blood)
Kidneys (blood)	Prostate (blood)	Urinary bladder wall (blood)
Liver (blood)	Salivary glands (blood)	Uterus (blood)
** The sub regions are only included in Rest of blood TIAC distribution if not specifically specified by user.*		

REST OF PARENCHYMA

The dynamic "Rest of parenchyma" source term can be used to distribute TIACs to subregions listed below, apportioned by mass. The subregions are only included in the TIAC allotment they have not been defined explicitly by user (see example in Appendix E). The masses used in this dynamic term for relative weighting are the subregion parenchyma masses. The specific masses used in the calculation depend on user-specified phantom selection, and can be reviewed in case save output file. Sex-specific source regions are used only for relevant sex.

Rest of parenchyma (dynamic source region based on weighted combination on parenchyma mass)		
Adipose tissue (par)	Gallbladder wall (par)	Salivary glands (par)
Adrenals (par)	Heart content (par)	Skin (par)
Bone - cortical volume (par)	Heart wall (par)	Small intestine wall (par)
Bone - trabecular volumes (par)	Kidneys (par)	
Bone marrow - red (active) (par)	Liver (par)	Spleen (par)
Bone marrow - yellow (inactive) (par)	Lungs (par)	Stomach wall (par)
Brain (par)	Lymph nodes - extrathoracic (par)	Teeth volume (par)
Breast tissue (par)	Lymph nodes - systemic (par)	Testes (par)
Cartilage (par)	Lymph nodes - thoracic (par)	Thymus (par)
Colon wall - left (par)	Major blood vessels (par)	Thyroid (par)
Colon wall - rectosigmoid (par)	Muscle (par)	Tongue (par)
Colon wall - right (par)	Oral mucosa (par)	Tonsils (par)
Esophagus wall (par)	Ovaries (par)	Ureters (par)
ET1 airway wall (par)	Pancreas (par)	Urinary bladder wall (par)
ET2 airway wall (par)	Pituitary gland (par)	
Eye lens (par)	Prostate (par)	Uterus (par)

** The sub regions are only included in Rest of* parenchyma *TIAC distribution if not specifically specified by user.*

APPENDIX E: EXAMPLE OF TIAC DISTRIBUTION IN *REST OF BODY* REGION

An example illustrating the process of the distribution of the *Rest of body* source TIAC as performed in calculations. When a user enters a TIAC into the *Rest of body* source region, that source gets distributed in a mass weighted fashion to the unaccounted for subregions. The bold percentages displayed in the central column indicate the mass-weighted portion of the *Rest of body* TIAC each subregion receives. This is displayed for informative purposes.

Phantom	ICRP Adult Female ♀		% injection accounted for	:	94%
Isotope	F-18		Assumed error in system	:	20%
Halflife	1.8295E+00	[hours]	# organs with nonzero TIACs	:	**6**
Subject ID	Sample "Rest of body" case		Input isotope/organ UID	:	HTS

Organ	User Entered TIAC	Total mass contribution [g]	% Total mass = % Rest of body				Final TIACs used for calcs
Adipose tissue	0	18996	**38.0%**	=	18996	/ 50047	0.6452
Adrenals	0	12	**0.0%**	=	12	/ 50047	0.0004
Bone - cortical volume	0	3075	**6.1%**	=	3075	/ 50047	0.1045
Bone - trabecular volumes	0	881	**1.8%**	=	881	/ 50047	0.0299
Bone marrow - red (active)	0	1143	**2.3%**	=	1143	/ 50047	0.0388
Bone marrow - yellow (inactive)	0	1500	**3.0%**	=	1500	/ 50047	0.0510
Brain	0.21	0	**0.0%**	=	0	/ 50047	0.2100
Breast tissue	0	337	**0.7%**	=	337	/ 50047	0.0114
Cartilage	0	948	**1.9%**	=	948	/ 50047	0.0322
Colon wall - left	0	155	**0.3%**	=	155	/ 50047	0.0053
Colon wall - rectosigmoid	0	72	**0.1%**	=	72	/ 50047	0.0025
Colon wall - right	0	155	**0.3%**	=	155	/ 50047	0.0053
Esophagus wall	0	38	**0.1%**	=	38	/ 50047	0.0013
ET1 airway wall	0	3	**0.0%**	=	3	/ 50047	0.0001
ET2 airway wall	0	3	**0.0%**	=	3	/ 50047	0.0001
Eye lens	0	0	**0.0%**	=	0	/ 50047	0.0000
Gallbladder wall	0	8	**0.0%**	=	8	/ 50047	0.0003
Heart content	0	330	**0.7%**	=	330	/ 50047	0.0112
Heart wall	0.11	0	**0.0%**	=	0	/ 50047	0.1100
Kidneys	0	318	**0.6%**	=	318	/ 50047	0.0108
Liver	0.13	0	**0.0%**	=	0	/ 50047	0.1300
Lungs	0.079	0	**0.0%**	=	0	/ 50047	0.0790
Lymph nodes - extrathoracic	0	12	**0.0%**	=	12	/ 50047	0.0004
Lymph nodes - systemic	0	117	**0.2%**	=	117	/ 50047	0.0040
Lymph nodes - thoracic	0	12	**0.0%**	=	12	/ 50047	0.0004
Major blood vessels	0	989	**2.0%**	=	989	/ 50047	0.0336
Muscle	0	17523	**35.0%**	=	17523	/ 50047	0.5952
Oral mucosa	0	25	**0.0%**	=	25	/ 50047	0.0008
Ovaries	0	8	**0.0%**	=	8	/ 50047	0.0003
Pancreas	0	125	**0.3%**	=	125	/ 50047	0.0043
Pituitary gland	0	1	**0.0%**	=	1	/ 50047	0.0000
Salivary glands	0	70	**0.1%**	=	70	/ 50047	0.0024
Skin	0	1962	**3.9%**	=	1962	/ 50047	0.0667
Small intestine wall	0	659	**1.3%**	=	659	/ 50047	0.0224
Spleen	0	182	**0.4%**	=	182	/ 50047	0.0062
Stomach wall	0	150	**0.3%**	=	150	/ 50047	0.0051
Teeth volume	0	36	**0.1%**	=	36	/ 50047	0.0012
Testes	0	0	**0.0%**	=	0	/ 50047	0.0000
Thymus	0	29	**0.1%**	=	29	/ 50047	0.0010
Thyroid	0	15	**0.0%**	=	15	/ 50047	0.0005
Tongue	0	58	**0.1%**	=	58	/ 50047	0.0020
Tonsils	0	3	**0.0%**	=	3	/ 50047	0.0001
Ureters	0	14	**0.0%**	=	14	/ 50047	0.0005
Urinary bladder content	0.26	0	**0.0%**	=	0	/ 50047	0.2600
Urinary bladder wall	0	37	**0.1%**	=	37	/ 50047	0.0013
Uterus	0	46	**0.1%**	=	46	/ 50047	0.0016
Rest of body	1.70						
sum	**2.489**	50047	**100.0%**				**2.489**

APPENDIX F: MIRDCALC PHANTOM MAKE UP (DESCRIPTION OF MASS-SCALING)

User Selected Phantom	Sex	Mass (Kg)	Phantom makeup				
ICRP 00 Newborn female	Female	4	100%	ICRP 00 Newborn female			
ICRP 01 year old female	Female	10	100%	ICRP 01 year old female			
ICRP 05 year old female	Female	19	100%	ICRP 05 year old female			
ICRP 10 year old female	Female	32	100%	ICRP 10 year old female			
ICRP 15 year old female	Female	53	100%	ICRP 15 year old female			
ICRP Adult Female	Female	60	100%	ICRP Adult Female			
ICRP 00 Newborn male	Male	4	100%	ICRP 00 Newborn male			
ICRP 01 year old male	Male	10	100%	ICRP 01 year old male			
ICRP 05 year old male	Male	19	100%	ICRP 05 year old male			
ICRP 10 year old male	Male	32	100%	ICRP 10 year old male			
ICRP 15 year old male	Male	56	100%	ICRP 15 year old male			
ICRP Adult Male	Male	73	100%	ICRP Adult Male			
05 kg (interp)	Female	5	77%	ICRP 00 Newborn female	&	23%	ICRP 01 year old female
05.5 kg (interp)	Female	6	69%	ICRP 00 Newborn female	&	31%	ICRP 01 year old female
06 kg (interp)	Female	6	62%	ICRP 00 Newborn female	&	38%	ICRP 01 year old female
06.5 kg (interp)	Female	6	54%	ICRP 00 Newborn female	&	46%	ICRP 01 year old female
07 kg (interp)	Female	7	46%	ICRP 00 Newborn female	&	54%	ICRP 01 year old female
07.5 kg (interp)	Female	8	38%	ICRP 00 Newborn female	&	62%	ICRP 01 year old female
08 kg (interp)	Female	8	31%	ICRP 00 Newborn female	&	69%	ICRP 01 year old female
08.5 kg (interp)	Female	8	23%	ICRP 00 Newborn female	&	77%	ICRP 01 year old female
09 kg (interp)	Female	9	15%	ICRP 00 Newborn female	&	85%	ICRP 01 year old female
09.5 kg (interp)	Female	10	8%	ICRP 00 Newborn female	&	92%	ICRP 01 year old female
10 kg (interp)	Female	10	100%	ICRP 01 year old female			
11 kg (interp)	Female	11	89%	ICRP 01 year old female	&	11%	ICRP 05 year old female
12 kg (interp)	Female	12	78%	ICRP 01 year old female	&	22%	ICRP 05 year old female
13 kg (interp)	Female	13	67%	ICRP 01 year old female	&	33%	ICRP 05 year old female
14 kg (interp)	Female	14	56%	ICRP 01 year old female	&	44%	ICRP 05 year old female
15 kg (interp)	Female	15	44%	ICRP 01 year old female	&	56%	ICRP 05 year old female
16 kg (interp)	Female	16	33%	ICRP 01 year old female	&	67%	ICRP 05 year old female
17 kg (interp)	Female	17	22%	ICRP 01 year old female	&	78%	ICRP 05 year old female
18 kg (interp)	Female	18	11%	ICRP 01 year old female	&	89%	ICRP 05 year old female
19 kg (interp)	Female	19	100%	ICRP 05 year old female			
20 kg (interp)	Female	20	92%	ICRP 05 year old female	&	8%	ICRP 10 year old female
21 kg (interp)	Female	21	85%	ICRP 05 year old female	&	15%	ICRP 10 year old female
22 kg (interp)	Female	22	77%	ICRP 05 year old female	&	23%	ICRP 10 year old female
23 kg (interp)	Female	23	69%	ICRP 05 year old female	&	31%	ICRP 10 year old female
24 kg (interp)	Female	24	62%	ICRP 05 year old female	&	38%	ICRP 10 year old female
25 kg (interp)	Female	25	54%	ICRP 05 year old female	&	46%	ICRP 10 year old female
26 kg (interp)	Female	26	46%	ICRP 05 year old female	&	54%	ICRP 10 year old female
27 kg (interp)	Female	27	38%	ICRP 05 year old female	&	62%	ICRP 10 year old female
28 kg (interp)	Female	28	31%	ICRP 05 year old female	&	69%	ICRP 10 year old female
29 kg (interp)	Female	29	23%	ICRP 05 year old female	&	77%	ICRP 10 year old female
30 kg (interp)	Female	30	15%	ICRP 05 year old female	&	85%	ICRP 10 year old female
31 kg (interp)	Female	31	8%	ICRP 05 year old female	&	92%	ICRP 10 year old female
32 kg (interp)	Female	32	100%	ICRP 10 year old female			
33 kg (interp)	Female	33	95%	ICRP 10 year old female	&	5%	ICRP 15 year old female
34 kg (interp)	Female	34	90%	ICRP 10 year old female	&	10%	ICRP 15 year old female
35 kg (interp)	Female	35	86%	ICRP 10 year old female	&	14%	ICRP 15 year old female
36 kg (interp)	Female	36	81%	ICRP 10 year old female	&	19%	ICRP 15 year old female
37 kg (interp)	Female	37	76%	ICRP 10 year old female	&	24%	ICRP 15 year old female
38 kg (interp)	Female	38	71%	ICRP 10 year old female	&	29%	ICRP 15 year old female
39 kg (interp)	Female	39	67%	ICRP 10 year old female	&	33%	ICRP 15 year old female
40 kg (interp)	Female	40	62%	ICRP 10 year old female	&	38%	ICRP 15 year old female
41 kg (interp)	Female	41	57%	ICRP 10 year old female	&	43%	ICRP 15 year old female
42 kg (interp)	Female	42	52%	ICRP 10 year old female	&	48%	ICRP 15 year old female
43 kg (interp)	Female	43	48%	ICRP 10 year old female	&	52%	ICRP 15 year old female
44 kg (interp)	Female	44	43%	ICRP 10 year old female	&	57%	ICRP 15 year old female
45 kg (interp)	Female	45	38%	ICRP 10 year old female	&	62%	ICRP 15 year old female
46 kg (interp)	Female	46	33%	ICRP 10 year old female	&	67%	ICRP 15 year old female
47 kg (interp)	Female	47	29%	ICRP 10 year old female	&	71%	ICRP 15 year old female
48 kg (interp)	Female	48	24%	ICRP 10 year old female	&	76%	ICRP 15 year old female
49 kg (interp)	Female	49	19%	ICRP 10 year old female	&	81%	ICRP 15 year old female

50 kg (interp)	Female	50	14%	ICRP 10 year old female	&	86%	ICRP 15 year old female
51 kg (interp)	Female	51	10%	ICRP 10 year old female	&	90%	ICRP 15 year old female
52 kg (interp)	Female	52	5%	ICRP 10 year old female	&	95%	ICRP 15 year old female
53 kg (interp)	Female	53	100%	ICRP 15 year old female			
54 kg (interp)	Female	54	86%	ICRP 15 year old female	&	14%	ICRP Adult Female
55 kg (interp)	Female	55	71%	ICRP 15 year old female	&	29%	ICRP Adult Female
56 kg (interp)	Female	56	57%	ICRP 15 year old female	&	43%	ICRP Adult Female
57 kg (interp)	Female	57	43%	ICRP 15 year old female	&	57%	ICRP Adult Female
58 kg (interp)	Female	58	29%	ICRP 15 year old female	&	71%	ICRP Adult Female
59 kg (interp)	Female	59	14%	ICRP 15 year old female	&	86%	ICRP Adult Female
60 kg (interp)	Female	60	0%	ICRP 15 year old female	&	100%	ICRP Adult Female
05 kg (interp)	Male	5	77%	ICRP 00 Newborn male	&	23%	ICRP 01 year old male
05.5 kg (interp)	Male	6	69%	ICRP 00 Newborn male	&	31%	ICRP 01 year old male
06 kg (interp)	Male	6	62%	ICRP 00 Newborn male	&	38%	ICRP 01 year old male
06.5 kg (interp)	Male	6	54%	ICRP 00 Newborn male	&	46%	ICRP 01 year old male
07 kg (interp)	Male	7	46%	ICRP 00 Newborn male	&	54%	ICRP 01 year old male
07.5 kg (interp)	Male	8	38%	ICRP 00 Newborn male	&	62%	ICRP 01 year old male
08 kg (interp)	Male	8	31%	ICRP 00 Newborn male	&	69%	ICRP 01 year old male
08.5 kg (interp)	Male	8	23%	ICRP 00 Newborn male	&	77%	ICRP 01 year old male
09 kg (interp)	Male	9	15%	ICRP 00 Newborn male	&	85%	ICRP 01 year old male
09.5 kg (interp)	Male	10	8%	ICRP 00 Newborn male	&	92%	ICRP 01 year old male
10 kg (interp)	Male	10	100%	ICRP 01 year old male			
11 kg (interp)	Male	11	89%	ICRP 01 year old male	&	11%	ICRP 05 year old male
12 kg (interp)	Male	12	78%	ICRP 01 year old male	&	22%	ICRP 05 year old male
13 kg (interp)	Male	13	67%	ICRP 01 year old male	&	33%	ICRP 05 year old male
14 kg (interp)	Male	14	56%	ICRP 01 year old male	&	44%	ICRP 05 year old male
15 kg (interp)	Male	15	44%	ICRP 01 year old male	&	56%	ICRP 05 year old male
16 kg (interp)	Male	16	33%	ICRP 01 year old male	&	67%	ICRP 05 year old male
17 kg (interp)	Male	17	22%	ICRP 01 year old male	&	78%	ICRP 05 year old male
18 kg (interp)	Male	18	11%	ICRP 01 year old male	&	89%	ICRP 05 year old male
19 kg (interp)	Male	19	100%	ICRP 05 year old male			
20 kg (interp)	Male	20	92%	ICRP 05 year old male	&	8%	ICRP 10 year old male
21 kg (interp)	Male	21	85%	ICRP 05 year old male	&	15%	ICRP 10 year old male
22 kg (interp)	Male	22	77%	ICRP 05 year old male	&	23%	ICRP 10 year old male
23 kg (interp)	Male	23	69%	ICRP 05 year old male	&	31%	ICRP 10 year old male
24 kg (interp)	Male	24	62%	ICRP 05 year old male	&	38%	ICRP 10 year old male
25 kg (interp)	Male	25	54%	ICRP 05 year old male	&	46%	ICRP 10 year old male
26 kg (interp)	Male	26	46%	ICRP 05 year old male	&	54%	ICRP 10 year old male
27 kg (interp)	Male	27	38%	ICRP 05 year old male	&	62%	ICRP 10 year old male
28 kg (interp)	Male	28	31%	ICRP 05 year old male	&	69%	ICRP 10 year old male
29 kg (interp)	Male	29	23%	ICRP 05 year old male	&	77%	ICRP 10 year old male
30 kg (interp)	Male	30	15%	ICRP 05 year old male	&	85%	ICRP 10 year old male
31 kg (interp)	Male	31	8%	ICRP 05 year old male	&	92%	ICRP 10 year old male
32 kg (interp)	Male	32	100%	ICRP 10 year old male			
33 kg (interp)	Male	33	96%	ICRP 10 year old male	&	4%	ICRP 15 year old male
34 kg (interp)	Male	34	92%	ICRP 10 year old male	&	8%	ICRP 15 year old male
35 kg (interp)	Male	35	88%	ICRP 10 year old male	&	13%	ICRP 15 year old male
36 kg (interp)	Male	36	83%	ICRP 10 year old male	&	17%	ICRP 15 year old male
37 kg (interp)	Male	37	79%	ICRP 10 year old male	&	21%	ICRP 15 year old male
38 kg (interp)	Male	38	75%	ICRP 10 year old male	&	25%	ICRP 15 year old male
39 kg (interp)	Male	39	71%	ICRP 10 year old male	&	29%	ICRP 15 year old male
40 kg (interp)	Male	40	67%	ICRP 10 year old male	&	33%	ICRP 15 year old male
41 kg (interp)	Male	41	63%	ICRP 10 year old male	&	38%	ICRP 15 year old male
42 kg (interp)	Male	42	58%	ICRP 10 year old male	&	42%	ICRP 15 year old male
43 kg (interp)	Male	43	54%	ICRP 10 year old male	&	46%	ICRP 15 year old male
44 kg (interp)	Male	44	50%	ICRP 10 year old male	&	50%	ICRP 15 year old male
45 kg (interp)	Male	45	46%	ICRP 10 year old male	&	54%	ICRP 15 year old male
46 kg (interp)	Male	46	42%	ICRP 10 year old male	&	58%	ICRP 15 year old male
47 kg (interp)	Male	47	38%	ICRP 10 year old male	&	63%	ICRP 15 year old male
48 kg (interp)	Male	48	33%	ICRP 10 year old male	&	67%	ICRP 15 year old male
49 kg (interp)	Male	49	29%	ICRP 10 year old male	&	71%	ICRP 15 year old male
50 kg (interp)	Male	50	25%	ICRP 10 year old male	&	75%	ICRP 15 year old male
51 kg (interp)	Male	51	21%	ICRP 10 year old male	&	79%	ICRP 15 year old male
52 kg (interp)	Male	52	17%	ICRP 10 year old male	&	83%	ICRP 15 year old male
53 kg (interp)	Male	53	13%	ICRP 10 year old male	&	88%	ICRP 15 year old male
54 kg (interp)	Male	54	8%	ICRP 10 year old male	&	92%	ICRP 15 year old male
55 kg (interp)	Male	55	4%	ICRP 10 year old male	&	96%	ICRP 15 year old male
56 kg (interp)	Male	56	100%	ICRP 15 year old male			
57 kg (interp)	Male	57	94%	ICRP 15 year old male	&	6%	ICRP Adult Male
58 kg (interp)	Male	58	88%	ICRP 15 year old male	&	12%	ICRP Adult Male

59 kg (interp)	Male	59	82%	ICRP 15 year old male	&	18%	ICRP Adult Male
60 kg (interp)	Male	60	76%	ICRP 15 year old male	&	24%	ICRP Adult Male
61 kg (interp)	Male	61	71%	ICRP 15 year old male	&	29%	ICRP Adult Male
62 kg (interp)	Male	62	65%	ICRP 15 year old male	&	35%	ICRP Adult Male
63 kg (interp)	Male	63	59%	ICRP 15 year old male	&	41%	ICRP Adult Male
64 kg (interp)	Male	64	53%	ICRP 15 year old male	&	47%	ICRP Adult Male
65 kg (interp)	Male	65	47%	ICRP 15 year old male	&	53%	ICRP Adult Male
66 kg (interp)	Male	66	41%	ICRP 15 year old male	&	59%	ICRP Adult Male
67 kg (interp)	Male	67	35%	ICRP 15 year old male	&	65%	ICRP Adult Male
68 kg (interp)	Male	68	29%	ICRP 15 year old male	&	71%	ICRP Adult Male
69 kg (interp)	Male	69	24%	ICRP 15 year old male	&	76%	ICRP Adult Male
70 kg (interp)	Male	70	18%	ICRP 15 year old male	&	82%	ICRP Adult Male
71 kg (interp)	Male	71	12%	ICRP 15 year old male	&	88%	ICRP Adult Male
72 kg (interp)	Male	72	6%	ICRP 15 year old male	&	94%	ICRP Adult Male
73 kg (interp)	Male	73			&	100%	ICRP Adult Male

APPENDIX G: EXAMPLES OF RISK INDEX CALCULATION

RISK INDEX CASE EXAMPLE #1:

Figure 1 corresponds to the output of MIRDcalc for the 1-year old female phantom, using the biokinetic model for the ^{18}F-FDG available in the ICRP 128 (Mattsson et al. 2015).

Risk Index (RI) (derived from O'Reilly et al, PMB, 2016) & Lifetime Attributable Risk (LAR) presented for Research use - derived from Radrat/Seer data (accessed 12/2020)															
NOTE - RI and LAR specific for phantom/biodistribution/age/sex. User can derive values from age-stratified table below. WARNING - TO COLLECT MULTIPLE AGES PROPERLY, RE-ENTER DATA FOR MULTIPLE RESPECTIVE PHANTOMS															
PHANTOM USED FOR DOSIMETRY	:	Female - ICRP 01 year old female													
SEX	:	Female													
AGE (yrs)	:	0	5	10	15	20	30	40	50	60	70	80	90	100	(usr) 1
RISK INDEX [%/MBq]	:	0.0149	0.0117	0.00934	0.00755	0.00613	0.00407	0.00365	0.00333	0.00296	0.00243	0.00175	0.000285	0.000278	0.0142
LAR [(case / 100k) /MBq]	:	6.13	4.85	3.87	3.13	2.53	1.67	1.47	1.26	0.986	0.624	0.281	0.024	0.0125	5.87

Figure 3: Example of output for the RI, female patient 18F-FDG.

The user may be aware that the values of LAR and RI are per administer activity (MBq). In order to obtain values for the desired age (for this case 2-year-old), the user must run MIRDcalc for the most proximal age of the available phantom, then by using a simple linear interpolation the specific values will be obtained. For instance, from the Figure 1 the user can find a LAR and RI of 5.6 case/100k/MBq and 0.0136 %/MBq respectively for a 2 years-old patient.

RIST INDEX CASE EXAMPLE #2:

For a male adult patient of 75 years-old who has been scanned with ^{99m}Tc-MAG3 to check the renal function, Figure 2 shows the output of MIRDcalc. The risk index obtained by linear interpolation is 0.00011 %/MBq and the LAR is 0.0351 case/100k/MBq.

Risk Index (RI) (derived from O'Reilly et al, PMB, 2016) & Lifetime Attributable Risk (LAR) presented for Research use - derived from Radrat/Seer data (accessed 12/2020)															
NOTE - RI and LAR specific for phantom/biodistribution/age/sex. User can derive values from age-stratified table below. WARNING - TO COLLECT MULTIPLE AGES PROPERLY, RE-ENTER DATA FOR MULTIPLE RESPECTIVE PHANTOMS															
PHANTOM USED FOR DOSIMETRY	:	Male - ICRP Adult Male													
SEX	:	Male													
AGE (yrs)	:	0	5	10	15	20	30	40	50	60	70	80	90	100	(usr) 40
RISK INDEX [%/MBq]	:	0.000677	0.000571	0.000485	0.000412	0.000351	0.000254	0.000248	0.000229	0.000188	0.000137	8.59E-05	8.24E-06	5.79E-06	0.000248
LAR [(case / 100k) /MBq]	:	0.327	0.278	0.236	0.2	0.171	0.125	0.122	0.113	0.0877	0.0508	0.0195	0.00101	0.000401	0.122

Figure 4: Example of output for the RI, male patient 99mTc-MAG3 (normal renal function)